NATIONAL POLAR-ORBITING OPERATIONAL ENVIRONMENTAL SATELLITE SYSTEM (NPOESS)

VIIRS OCEAN COLOR/CHLOROPHYLL ALGORITHM THEORETICAL BASIS DOCUMENT (D43763 Rev A)

CDRL No. A032

Northrop Grumman Space & Mission Systems Corporation
One Space Park
Redondo Beach, California 90278

This document has been identified per the NPOESS Common Data Format Control Book – External Volume 5 Metadata, D34862-05, Appendix B as a document to be provided to the NOAA Comprehensive Large Array-data Stewardship System (CLASS) via the delivery of NPOESS Document Release Packages to CLASS.

The information provided herein does not contain technical data as defined in the International Traffic in Arms Regulations (ITAR) 22 CFR 120.10.

This document has been approved by the Unites States Government for public release in accordance with NOAA NPOESS Integrated Program Office.

NATIONAL POLAR-ORBITING OPERATIONAL ENVIRONMENTAL SATELLITE SYSTEM (NPOESS)

VIIRS OCEAN COLOR/CHLOROPHYLL ALGORITHM THEORETICAL BASIS DOCUMENT (D43763 Rev A)

ELECTRONIC APPROVAL SIGNATURES:

_____

Roy Tsugawa   Date
Algorithm & Data Processing IPT Lead &
Algorithm Change Control Board Chairperson

_____

Ben James   Date
Operations & Support IPT Lead

The following individuals are recognized for their contributions to the current or previous versions of this document.

    Kendal Carder
    Corinne Carter
    Dorlisa Hommel
    Justin Ip
    Quanhua Liu

TABLE OF CONTENTS

LIST OF FIGURES

LIST OF TABLES

GLOSSARY OF ACRONYMS

ATBD	Algorithm Theoretical Basis Document
Case 1	Water whose optically active constituents are totally correlated
Case 2	Water whose optically active constituents are totally uncorrelated
CZCS	Coastal Zone Color Scanner
DOM	Dissolved Organic Matter
EDR	Environmental Data Record
IOP	Inherent Optical Properties
MODIS	Moderate-Resolution Imaging Spectroradiometer
NDT	Nitrate Depletion Temperature
NEdN	Noise-Equivalent Delta Radiance
NIR	Near InfraRed
RMS	Root mean square
SeaBAM	SeaWiFS Bio-optical Algorithm Mini-workshop
SeaWiFS	Sea-viewing Wide Field-of-view Sensor
SDR	Sensor Data Record
SPM	Suspended Particulate Matter
SRD	Sensor Requirements Documents
SST	Sea Surface Temperature
SZA	Solar Zenith Angle
TOA	Top of Atmosphere
VIIRS	Visible/Infrared Imager/Radiometer Suite

GLOSSARY OF SYMBOLS

A	The absorption coefficient
$a_i(\lambda)$	Wavelength-dependent parameters in phytoplankton pigment absorption parameterization
A_i	Empirical coefficients
b_b	The backscattering coefficient
B	Empirical coefficient
C	Chlorophyll a concentration
C_i	Concentration of i-th substance
E	Irradiance
$F(C_i)$	The objective function to be minimized
k	The DOM spectral absorption slope
L_w	Water-leaving radiance
n	The backscatter spectral ratio exponent
Q	The Q-factor
r	Spectral reflectance ratio
$r_{1,2}$	Relative errors of retrieving
R	Diffuse reflectance, i.e., the ratio of the upwelling irradiance to the downwelling irradiance just beneath the sea surface
R_{rs}	Remote-sensing reflectance, i.e., the ratio of water-leaving radiance to the downwelling irradiance just above the sea surface
X_i	Empirical coefficients
Y_i	Empirical coefficients
t	Transmittance
λ	Wavelength
θ	Zenith angle
$\sigma(\lambda)$	A weighting function

ABSTRACT

The Ocean Color/Chlorophyll (OCC) EDR contains chlorophyll a concentration, Ocean Color (Normalized Water-Leaving Radiance, nLw), Inherent Optical Properties of Absorption (IOP-a), and Inherent Optical Properties of Scattering (IOP-s) that are retrieved from remote sensing reflectance $R_{rs}(\lambda)$ in the five visible wavelength bands (M1 to M5) of the Visible/Infrared Imager/Radiometer Suite (VIIRS). The $R_{rs}(\lambda)$ is defined as the water-leaving radiance divided by the downwelling irradiance just above the sea surface, and are determined from measured top-of-atmosphere (TOA) radiances by the VIIRS atmospheric correction over ocean (ACO) algorithm. We use the Case 2 chlorophyll a algorithm developed by Carder *et al.* (2003, 2004) for use on MODIS data. This algorithm is based on a semi-analytical, bio-optics model of $R_{rs}(\lambda)$. The model has two free parameters—the absorption coefficient due to phytoplankton at 675 nm, $a_{ph}(675)$, and the absorption coefficient due to gelbstoff at 400 nm, $a_g(400)$. The model has many other parameters that are fixed, or are specified based on the region and season of the VIIRS scene.

$R_{rs}(\lambda)$ values at 412, 445, 488, 555, and 672 wavelengths are retrieved from the VIIRS ACO algorithm and put into the Carder bio-optics model. The model is inverted and $a_{ph}(675)$ and $a_g(400)$ are computed. Chlorophyll a concentration is then derived simply from the $a_{ph}(675)$ value. The algorithm also outputs the nLw, the IOP-a and IOP-s at the five visible VIIRS wavelengths. The VIIRS sea surface temperature (SST) and seasonal global nitrate depletion temperature (NDT) data (as used in MODIS) are the additional inputs. The algorithm uses the difference in SST and NDT for setting five different sets of model parameters according to the latest branching and weighting strategy employed in MODIS (SeaDAS). In highly turbid waters, an empirical $R_{rs}(488)/R_{rs}(555)$ ratio algorithm is used instead of the $R_{rs}(\lambda)$ model to estimate chlorophyll concentration.

1.0   INTRODUCTION

1.1   PURPOSE

This Algorithm Theoretical Basis Document (ATBD) describes the algorithm used to retrieve ocean color and chlorophyll *a* concentration, a VIIRS Level 2 product, contained in the Ocean Color/Chlorophyll EDR. Chlorophyll concentration is measured in mg/m^3 units and retrieved from remote sensing reflectance. This document describes the physical theory and mathematical background of the algorithm, provides implementation details, and identifies assumptions and limitations of the adopted approach.

1.2   SCOPE

This document covers the algorithm theoretical basis for the retrieval of ocean color and chlorophyll *a* concentration from remote sensing reflectance. Section 1 describes the purpose and scope of the document. Section 2 provides an experiment overview. The algorithm description is presented in Section 3. Section 4 summarizes assumptions and limitations. References for publications cited in the text are given in Section 5.

1.3   VIIRS DOCUMENTS

References to VIIRS documents are indicated by #Y numbers in italicized brackets, e.g., *[#Y2408]*.

[# Y1296]   VIIRS Sensor Requirements Document, Technical Requirements Document, 1997.

[#Y2408] Ocean Color/Chlorophyll Visible/Infrared Imager/radiometer Suite Algorithm Theoretical Basis Document, Version 7, 2005

[# Y2411]   SBRS Document, Version 5, 2002

[# Y2476]   VIIRS Ocean Module Level Software Architecture Document

[# Y3227]   VIIRS Ocean Color Unit Level Detailed Design Document

[#PS154640-101A]   VIIRS Sensor Specification Document

1.4   REVISIONS

The first version of this document was completed in October 1998. The second version was dated June 1999. The third version was completed in May 2000. The fourth version of this document, dated May 2001, included additions to the Algorithm Input section, a table added to section 2.2 describing the VIIRS bands used in the SDR, and a table added to section 3.2.1 which describes the flags used to generate the level 2 product. This is the fifth version of this document. The lists of flags and VIIRS bands have both been updated. Additionally, section 3.3.4 has been added which describes the latest model branching and weighting strategy of the chlorophyll retrieval algorithms using VIIRS skin SST and MODIS NDT data as input.

2.0   EXPERIMENT OVERVIEW

2.1   OBJECTIVES OF OCEAN COLOR/CHLOROPHYLL RETRIEVALS

The required Environmental Data Record (EDR) is the concentration of chlorophyll in a vertical column of the surface layer in the ocean. Ocean color, as measured by the radiance reflected by the ocean in a number of narrow visible bands, is used to infer chlorophyll concentration [*# Y1296*]. The main objectives of chlorophyll retrievals are:

- To provide the scientific community with operational data for quantification of the ocean's role in the global carbon cycle and other biogeochemical cycles

- To acquire global data on marine optical properties with emphasis on frontal zones and eddies

- To identify bioluminescence potential in different ocean areas.

With respect to remote sensing, two main types of seawater have been defined (Morel and Prieur, 1977; Gordon and Morel, 1983). Case 1 waters are characterized by a strong correlation between scattering and absorbing substance concentrations and the chlorophyll a concentration. The open ocean surface water is typical Case 1 water. The strong correlation is due to the fact that all the substances originate in biological processes. A primary source of the substances is photosynthesis of marine phytoplankton. Case 1 waters can be characterized by a single parameter—chlorophyll concentration. Case 2 waters are characterized by a lack of any correlation between scattering and absorbing substance concentrations and chlorophyll *a* concentration. Coastal waters are often referred to as Case 2 waters. Marine phytoplankton is not the dominant, optically active water substance. Particulate matter and colored dissolved organic matter (DOM), which do not always co-vary with chlorophyll, also affect seawater optical properties. Case 2 water can be referred to as multi-parameter water; its optical properties are described by a set of parameters. It must be acknowledged that this classification concept is somewhat idealized because, in reality, all waters belong to an intermediate case.

2.2   INSTRUMENT CHARACTERISTICS

The retrieval of ocean color EDR is based on bio-optical algorithms using the spectral reflectance of the seawater column in the visible spectral region. VIIRS has five spectral bands in the visible region [*Table-1*]. Bandwidths are equal to 18 nm for the second band and 20 nm for other bands. These bands have SeaWiFS and MODIS heritage. Table 1 gives the VIIRS bands used in the SDR and EDRs. The bio-optical algorithms retrieve the Ocean Color/Chlorophyll EDR from remote sensing reflectance of seawater that is the output of atmospheric correction algorithms. The atmospheric correction algorithms make use of near infrared (NIR) bands. VIIRS has two NIR bands. They are located at wavelengths 746 and 865 nm. Their bandwidths are 15 and 39 nm respectively. In contrast to SeaWiFS, the first VIIRS NIR band was shifted and narrowed to avoid oxygen absorption at 762 nm. The SeaWiFS NIR band at 765 nm includes the 762 nm oxygen absorption band. Possible interaction between oxygen absorption and scattering of thin cirrus clouds significantly degrades the performance of the SeaWiFS atmospheric correction.

Table 1. VIIRS Bands Used to Process the Ocean Color EDR.

VIIRS Band name	Wavelength (nm)	Bandwidth (nm)	L_{typ} (W/m^2/μm/sr)	Primary use
M1	412	20	44.9	Dissolved organic matter (including Gelbstoff), absorbing aerosols
M2	445	18	40	Chlorophyll absorption
M3	488	20	32	Pigment absorption (Case 2 waters)
M4	555	20	21	Pigments, optical properties, sediment
M5	672	20	10	Atmospheric correction and sediments
M6	746	15	9.6	Atmospheric correction, aerosol reflectance
M7	865	39	6.4	Atmospheric correction, aerosol reflectance.

2.2   SYSTEM REQUIREMENT

The system requirement for Ocean Color/Chlorophyll is listed in Section 40.7.6 of the NPOESS System Specification, SY15-0007_N_NPOESS System Specification.doc. It is stated,

Ocean color is defined as the spectrum of normalized water-leaving radiances (nL$_w$). All geophysical quantities of interest, e.g., the concentration of phytoplankton pigment chlorophyll α (chlorophyll-α) and the inherent optical properties of absorption and scattering of surface waters (ocean optical properties), are derived from these nL$_w$ values. Normalized water-leaving radiances are measured in W m^{-2} μm^{-1} sr^{-1}. Ocean optical properties, absorption, and scattering are estimated at each measured visible wavelength, and have units of m^{-1} while chlorophyll-α is measured in mg m^{-3}. This EDR is required under "clear, daytime conditions" only. "Clear" for this EDR is a cloud mask indicator of "confidently clear" for the horizontal cell of interest, and if the thin cirrus detection flag is not set for that horizontal cell. Day condition for this EDR is when the solar zenith angle is less than 70 deg and when the cloud mask does not indicate that the cell of interest is in shadow. This EDR will be produced under "probably clear" or "probably cloudy" conditions indicated by the cloud mask or under Exclusion conditions, except for Ice Covered Oceans Exclusion, but without performance specifications.

<u>Units</u>: Ocean Color: W m^{-2} μm^{-1} sr^{-1}, Ocean Optical Properties: m^{-1}, Chlorophyll: mg m^{-3}

Paragraph	Subject	Specified Value
	a. Horizontal Cell Size	
40.7.6-1	1. Worst Case	1.3 km
40.7.6-2	2. Nadir	0.75 km
40.7.6-3	b. Horizontal Reporting Interval	HCS
40.7.6-29	c. Horizontal Coverage	Oceans
	d. Measurement Range	
40.7.6-13	1. Ocean Color	0.1 - 40 W m^{-2} micrometer^{-1} sr^{-1}

Paragraph	Subject	Specified Value
40.7.6-14	2. Optical Properties, Absorption	0.01 - 10 m^{-1}
40.7.6-15	3. Optical Properties, Scattering	0.01 - 50 m^{-1}
40.7.6-6	4. Optical Properties, Chlorophyll	0.05 - 50 mg/m^3
	e. Measurement Accuracy	
40.7.6-17	1. Ocean Color, Operational	Greater of 10% or 0.1 W m^{-2} micrometer^{-1} sr^{-1}
40.7.6-19	2. Optical Properties, Operational	40%
40.7.6-7a	3. Chlorophyll, Operational, Chl < 1.0 mg/m3	40%
40.7.6-7b	4. Chlorophyll, Operational, 1.0 mg/m3 < Chl < 10 mg/m3	40%
40.7.6-7c	5. Chlorophyll, Operational, Chl > 10 mg/m3	50%
	f. Measurement Precision	
40.7.6-22	1. Ocean Color, Operational	Greater of 5% or 0.05 W m^{-2} micrometer^{-1} sr^{-1}
40.7.6-24	2. Optical Properties, Operational	20%
40.7.6-8a	3. Chlorophyll, Operational, Chl < 1.0 mg/m3	20%
40.7.6-8b	4. Chlorophyll, Operational, 1.0 mg/m3 < Chl < 10 mg/m3	30%
40.7.6-8c	5. Chlorophyll, Operational, Chl > 10 mg/m3	50%
	g. Mapping Uncertainty, 3 Sigma	
40.7.6-9	1. Worst Case	1.5 km
40.7.6-10	2. Nadir	0.4 km
40.7.6-11	h. Max Local Average Revisit Time	24 hrs
40.7.6-26	i. Long Term Stability (W m^{-2} micrometer^{-1} sr^{-1}) (C) SEE NOTE 1	Max Chl Absorption 0.5, Min Chl Absorption 0.25, Atmospheric Correction 0.08
40.7.6-27	j. Latency, Operational	NPP - 140 min. NPOESS - 28 min.
40.7.6-31a	l. Degradation Condition: Shallow water less than 50 m	(SYS-TBR-024)
	k. Excluded Measurement Conditions	
40.7.6-30a	1. Strongly Absorbing Aerosols With Single Scattering Albedo ω0(555) < 0.7	
40.7.6-30b	2. Dissolved Organic Matter Absorption Dominant Waters, DOM Absorption a(410) > 2m^{-1}	
40.7.6-30c	3. Very Turbid Coastal Waters, Mass Loading > 60 mg/l	
40.7.6-30d	4. Sun Glint < 36 deg	
40.7.6-30e	5. Orbit Other Than Nominal 1330 Orbit	
40.7.6-30f	6. With scattering error greater than would exist at a point 12 milliradians away from the VIIRS Bright Target	
40.7.6-30g	7. Beyond a Swath Width of 1700 km	
40.7.6-30h	8. Aerosol Optical Thickness > 0.3	
40.7.6-30i	9. Over ocean with calcite concentration due to coccolithophores greater than or equal to 0.3 mg/m^3.	
40.7.6-30j	10. Ice-covered oceans	

Note 1: Stability is for normalized water-leaving radiance at the band of Maximum Chlorophyll absorption (measured at approximately 445 nm), Min Chlorophyll Absorption (at approximately 555 nm), and Atmospheric Correction (at approximately 865 nm).

3.0 ALGORITHM DESCRIPTION

3.1 OVERVIEW AND BACKGROUND

All algorithms for retrieval of seawater constituents from spectral reflectance (or water color spectrum) can be divided into two main groups. The first group is referred to as empirical algorithms. They are based on the empirical correlation between radiance band ratios and water constituent concentrations. The radiance band-ratio methods for determining the phytoplankton pigment concentration have been shown to be useful in global mapping of the ocean phytoplankton pigments (Gordon *et al.,* 1983).

A typical example of the empirical approach is the CZCS basic algorithm (Gordon *et al.,* 1983):

$$\log C_1 = 0.053 - 1.71\log(r(1,3)) \ \text{ if } \ C_1 < 1.5 \ \text{ or } \ C_1 > 1.5 \ \text{ but } \ C_2 < 1.5 \qquad (1)$$

$$\log C_2 = 0.522 - 2.44\log(r(2,3)) \ \text{ if } \ C_1 > 1.5 \ \text{ and } \ C_2 > 1.5$$

where C_1 or C_2 is the total pigment concentration, i.e., the sum of the concentrations of chlorophyll *a* and phaeopigments, and $r(1,3) = L_w(443)/L_w(550)$, $r(2,3) = L_w(520)/L_w(550)$ are ratios of water-leaving radiances in CZCS spectral bands. Pigment retrievals from CZCS data in Case 1 waters have achieved reasonable results, i.e., accuracy within ±40% for best cases. However, the retrieval of pigment concentration may be less than 100 percent accurate for Case 2 waters (Carder *et al.,* 1991).

The SeaWiFS basic chlorophyll *a* algorithm is another example of an empirical approach. It is expressed as a cubic polynomial (O'Reilly *et al.,* 1998):

$$\log(C - C_0) = A_0 + A_1 r + A_2 r^2 + A_3 r^3 \qquad (2)$$

where C_0 and A_i , *i*=0,1,2,3, are empirical coefficients, and r=log[R_{rs}(488)/R_{rs}(555)]. R_{rs} is remote-sensing reflectance, the ratio of water-leaving radiance to downwelling irradiance just above the sea surface. The new coefficients for the SeaWiFS chlorophyll *a* algorithm (as of September 1998) are: C_0 = −0.0929 mg/m^3, A_0 = 0.2974, A_1 = −2.2429, A_2 = 0.8358, A_3 = −0.0077 (Maritorena, 1998).

A newer OC-4 SeaWiFS empirical algorithm has been developed by O'Reilly, (2000).

These simple empirical algorithms are not reliable for Case 2 coastal waters. In such cases the second group, so-called analytical (or semi-analytical) algorithms, may be promising. Analytical algorithms use a reflectance model as well as a spectral model of the inherent optical properties (IOPs). The IOPs of water constituents are derived from inversion of the reflectance model. The inversion of the reflectance model can be performed either by direct solution of reflectance model equations or by minimization of the spectral difference between measured and modeled reflectance spectra:

$$F(C_j) = \sum_i \left[R_{i\,measured} - R_i(C_j) \right]^2 / \sigma_i^2 \qquad (3)$$

where $F(C_j)$ is the objective function, $R_i = R(\lambda_i)$ is the modeled spectral reflectance, C_j is the water constituent concentrations, and $\sigma_i = \sigma(\lambda_i)$ is the spectral weighting function.

There have been many applications of the analytical algorithms to the retrieval of the water optical properties and constituent concentrations since 1985 (Burenkov *et al.,* 1985; Sugihara *et al.,* 1985; Carder *et al.,* 1991; Lee *et al.,* 1994; Doerffer and Fischer, 1994; Roesler and Perry, 1995; Hoge and Lyon, 1996; Vasilkov, 1997; Garver and Siegel, 1997). Minimization of the nonlinear function (Equation 3) was used in Burenkov *et al.* (1985), Lee *et al.* (1994), Doerffer and Fischer (1994), Roesler and Perry (1995), and Garver and Siegel (1997). The minimization of a nonlinear function of several variables may be computationally expensive and, if so, it cannot be used for operational purposes. An alternative approach is based on a direct inversion technique. The radiance model is transformed into an equation set with unknowns related to water constituent concentrations. Two nonlinear equations are used by Carder *et al.* (1991) to derive the absorption coefficients of chlorophyll and non-co-varying DOM. An exact linear matrix inversion of a seawater radiance model was recently proposed in Hoge and Lyon (1996). The least-squares technique to solve an over-determined system of linear equations was used by Sugihara *et al.* (1985) and Vasilkov (1997).

The algorithm described in the present document is based on the approach of Carder *et al.* (1991) and its modification used for the MODIS Case 2 chlorophyll *a* algorithm (Carder *et al.,* 2003). The algorithm description in the present document is a brief version of Carder *et al.* (2003) with necessary modifications for VIIRS.

3.2   ALGORITHM INPUT

3.2.1   Masks and Flags

The RSR IP contains the remote sensing reflectances. There are three masks that are used on RSR data and they are the cloud/ice mask, water/land mask, and sun glint mask. Table 2a and 2b defines the pixel and granule level quality flags that are used for the ocean color EDR data product. The level 2 data product is the Ocean Color/Chlorophyll EDR and contains the Chlorophyll *a* concentration, and nLw, IOP-a, IOP-s at the five VIIRS ocean bands, and the set of granule and pixel level quality flags.

Table 2a Pixel level quality flag structure for the Ocean Color EDR.

BYTE	Bit	Flag Description Key	Bit Value
0	0	Ocean Color quality at M1	0 = Good, 1 = Poor
	1	Ocean Color quality at M2	0 = Good, 1 = Poor
	2	Ocean Color quality at M3	0 = Good, 1 = Poor
	3	Ocean Color quality at M4	0 = Good, 1 = Poor
	4	Ocean Color quality at M5	0 = Good, 1 = Poor
	5	Chlorophyll Concentration quality	0 = Good, 1 = Poor
	6	IOP-a quality at M1	0 = Good, 1 = Poor
	7	IOP-s quality at M1	0 = Good, 1 = Poor
1	0	IOP-a quality at M2	0 = Good, 1 = Poor
	1	IOP-s quality at M2	0 = Good, 1 = Poor
	2	IOP-a quality at M3	0 = Good, 1 = Poor
	3	IOP-s quality at M3	0 = Good, 1 = Poor
	4	IOP-a quality at M4	0 = Good, 1 = Poor
	5	IOP-s quality at M4	0 = Good, 1 = Poor
	6	IOP-a quality at M5	0 = Good, 1 = Poor
	7	IOP-s quality at M5	0 = Good, 1 = Poor
2	0	SDR Quality for Ocean Bands M1 to M7	0 = Good for all 7 bands 1 = Poor (any band greater than thresholds)
	1	Input Total Ozone Column Quality	0 = Good, 1 = Poor
	2	Wind Speed Indicator	0 = Low wind ($0 \leq$ speed ≤ 8.0 m/s) 1 = High wind (speed > 8.0 m/s)
	3	Epsilon Out of Aerosol Models Range	0 = Within model range ($0.85 \leq \varepsilon \leq 1.35$) 1 = Out of model range, or no ε available

BYTE	Bit	Flag Description Key	Bit Value
	4-6	Atmospheric Correction Failure	000 = Atmospheric correction successful 001 = Ozone correction failure 010 = Whitecap correction failure 011 = Polarization correction failure 100 = Rayleigh correction failure 101 = Aerosol correction failure 110 = Zero diffuse transmittance 111 = No correction possible
	7	Spare	Set to 0
3	0-1	Land/water	00 = Sea water, 01 = Coastal water, 10 = Inland water, 11 = Land
	2	Snow/Ice	0 = Not snow/ice 1 = Snow/ice
	3	Day/Night Exclusion	0 = Day (SZA $\leq$ 70°) 1 = Night (SZA > 70°) exclusion
	4	Sun Glint Exclusion	0 = No sun glint, 1 = Sun glint
	5	Horizontal Reporting Interval (HRI) > 1.3 km Exclusion	0 = No, Nadir to 1.3 km (0° $\leq$ Sensor Zenith Angle $\leq$ 50.3^o) 1 = Yes, HRI > 1.3 km exclusion
	6	Shallow Water	0 = Deep water (Depth $\geq$ 50 m) 1 = Shallow water (Depth < 50 m)
	7	Stray Light Maximum Radiance Exclusion	0 = No exclusion, or no mask available 1 = Stray light exclusion
4	0-1	Cloud Confident Indicator	00 = Confident clear, 01 = Probably clear 10 = Probably cloudy, 11 = Confident cloudy
	2	Adjacent Pixel Cloud Confident Indicator	0 = Confident clear, 1 = Cloudy
	3	Cirrus Cloud Detection	0 = No Cirrus detected 1 = Cirrus detected
	4	Cloud Shadow Exclusion	0 = No cloud shadow, 1 = Shadow present

BYTE	Bit	Flag Description Key	Bit Value
	5	Non Cloud Obstruction (Heavy Aerosol)	0 = No, 1 = Yes
	6	Strongly Absorbing Aerosol (Single Scattering Albedo ω_0(M4) < 0.7) Exclusion	0 = No exclusion, or no ω_0(M4) available 1 = Strongly absorbing aerosol present (ω_0(M4) < 0.7)
	7	Aerosol Optical Thickness (AOT @ M7) Exclusion (AOT > 1.0)	0 = No AOT exclusion, or no AOT available 1 = AOT exclusion (AOT > 1.0)
5	0	Turbid Water (R_{rs}(M5) > 0.012) Exclusion	0 = No (R_{rs}(M5) $\leq$ 0.012), or no R_{rs}(M5) available 1 = Yes (R_{rs}(M5) > 0.012)
	1	Over ocean with calcite concentration due to coccolithophores greater than or equal to 0.3 mg/m^3	0 = No coccolithophores, or no information 1 = Yes (nLw(M2) $\geq$ 1.1 & nLw(M4) $\geq$ 0.81 & L_{aer}(M6) $\leq$ 1.1 & 0.6 $\leq$ nLw(M2)/ nLw(M4) $\leq$ 1.1)
	2	Dissolved Organic Matter Absorption Dominant Waters Exclusion (DOM absorption a(410) > 2/m)	0 = No DOM absorption exclusion, or no a(410) available 1 = DOM absorption exclusion (a(410) > 2/m)
	3-4	Range of Chlorophyll Concentration	00 = No chlorophyll retrieval 01 = Chlorophyll < 1 mg/m^3 10 = 1.0 $\leq$ Chlorophyll < 10 mg/m^3 11 = Chlorophyll $\geq$ 10 mg/m^3
	5-7	OCC Algorithm Branching	001 = Carder empirical algorithm 010 = Unpackaged phytoplankton model 011 = Weighted global-unpackaged algorithm 100 = Weighted packaged-global algorithm 101 = Weighted fully packaged-packaged 110 = Fully packaged phytoplankton model 111 = No OCC retrieval
6	0	Ocean Color (any band) Out of Reporting Range	0 = In range (1.0 $\leq$ nLw $\leq$ 40 W/m^2/μm/sr) 1 = Out of range
	1	Chlorophyll Concentration Out of Reporting Range	0 = In range (0.05 $\leq$ Chl $\leq$ 50 mg/m^3) 1 = Out of range
	2	IOP-a (any band) Out of Reporting Range	0 = In range (0.01 $\leq$ IOP_a $\leq$ 10 /m) 1 = Out of range

BYTE	Bit	Flag Description Key	Bit Value
	3	IOP-s (any band) Out of Reporting Range	0 = In range (0.01 $\leq$ IOP_s $\leq$ 50 /m) 1 = Out of range
	4	Input skin SST EDR Quality	0 = Good, 1 = Poor
	5	Spare	Set to 0
	6	Spare	Set to 0
	7	Spare	Set to 0

Table 2b Granule level quality flag structure for the Ocean Color EDR.

Input	Type	Description/Source	Units/Range
Overall Ocean Color Quality at M1	Integer	Percent of high quality Ocean Color retrievals at M1 / Ocean Color/Chlorophyll EDR	0 % to 100 %
Overall Ocean Color Quality at M2	Integer	Percent of high quality Ocean Color retrievals at M2 / Ocean Color/Chlorophyll EDR	0 % to 100 %
Overall Ocean Color Quality at M3	Integer	Percent of high quality Ocean Color retrievals at M3 / Ocean Color/Chlorophyll EDR	0 % to 100 %
Overall Ocean Color Quality at M4	Integer	Percent of high quality Ocean Color retrievals at M4 / Ocean Color/Chlorophyll EDR	0 % to 100 %
Overall Ocean Color Quality at M5	Integer	Percent of high quality Ocean Color retrievals at M5 / Ocean Color/Chlorophyll EDR	0 % to 100 %
Overall Chlorophyll a Concentration Quality	Integer	Percent of high quality Chlorophyll Concentration retrievals / Ocean Color/Chlorophyll EDR	0 % to 100 %
Overall IOP-a Quality at M1	Integer	Percent of high quality IOP-a retrievals at M1 / Ocean Color/Chlorophyll EDR	0 % to 100 %
Overall IOP-a Quality at M2	Integer	Percent of high quality IOP-a retrievals at M2 / Ocean Color/Chlorophyll EDR	0 % to 100 %
Overall IOP-a Quality at M3	Integer	Percent of high quality IOP-a retrievals at M3 / Ocean Color/Chlorophyll EDR	0 % to 100 %
Overall IOP-a Quality at M4	Integer	Percent of high quality IOP-a retrievals at M4 / Ocean Color/Chlorophyll EDR	0 % to 100 %
Overall IOP-a Quality at M5	Integer	Percent of high quality IOP-a retrievals at M5 / Ocean Color/Chlorophyll EDR	0 % to 100 %
Overall IOP-s Quality at M1	Integer	Percent of high quality IOP-s retrievals at M1 / Ocean Color/Chlorophyll EDR	0 % to 100 %
Overall IOP-s Quality at M2	Integer	Percent of high quality IOP-s retrievals at M2 / Ocean Color/Chlorophyll EDR	0 % to 100 %

Input	Type	Description/Source	Units/Range
Overall IOP-s Quality at M3	Integer	Percent of high quality IOP-s retrievals at M3 / Ocean Color/Chlorophyll EDR	0 % to 100 %
Overall IOP-s Quality at M4	Integer	Percent of high quality IOP-s retrievals at M4 / Ocean Color/Chlorophyll EDR	0 % to 100 %
Overall IOP-s Quality at M5	Integer	Percent of high quality IOP-s retrievals at M5 / Ocean Color/Chlorophyll EDR	0 % to 100 %
Input SDR Quality	Integer	Percent of high quality VIIRS SDR data input / VIIRS SDR	0 % to 100 %
Input SST Quality	Integer	Percent of high quality VIIRS SST data input / VIIRS SST EDR	0 % to 100 %
Summary Ocean Color Range Check	Integer	Percent of all Ocean Color retrievals (all bands) that are out of expected range / Ocean Color/Chlorophyll EDR	0 % to 100 %
Summary Chlorophyll Concentration Range Check	Integer	Percent of Chlorophyll Concentration retrievals that are out of expected range / Ocean Color/Chlorophyll EDR	0 % to 100 %
Summary IOP-a Range Check	Integer	Percent of IOP-a retrievals that are out of expected range / Ocean Color/Chlorophyll EDR	0 % to 100 %
Summary IOP-s Range Check	Integer	Percent of IOP-s retrievals that are out of expected range / Ocean Color/Chlorophyll EDR	0 % to 100 %
No Day Pixel in Granule	Integer	Indicates whether any day pixels are in the current granule / Solar zenith angles	0 = Day pixels in granule 1 = No day pixels in granule
Exclusion Summary	Integer	Percent of pixels have one or more exclusion conditions	0 % to 100 %
No Ocean Coverage	Integer	Granule No Ocean flag / VIIRS Cloud Mask IP	0 = ocean 1 = no ocean

3.2.2 VIIRS Data

Remote sensing reflectances in four VIIRS visible bands (412, 445, 488, and 555 nm) are required as inputs for the chlorophyll retrieval algorithm. The remote sensing reflectances are the output from the atmospheric correction algorithm. VIIRS sea surface temperature EDR and nitrate depletion temperature are used as an indicator of the degree of pigment packaging. This is described in further detail in section 3.3.4.

3.2.3 Non-VIIRS Data

The chlorophyll algorithm also requires nitrate depletion temperature data for determine model branching and weighting. Non-VIIRS data sets are also needed for the atmospheric correction algorithm. They include total ozone amount, atmospheric pressure, and surface wind speed.

3.3 THEORETICAL DESCRIPTION OF CHLOROPHYLL ALGORITHM

3.3.1 Radiance and Seawater Optical Properties Models

Many approaches exist to obtain an approximate solution to the radiative transfer equation, which can serve as the marine reflectance model (Gordon, 1973; Golubitskiy and Levin, 1980; Zaneveld, 1982; Aas, 1987; and Haltrin and Kattawar, 1993). They are based on two main physical properties of seawater: First, scattering is highly anisotropic in the forward direction; and second, seawater is an absorbing medium. They give roughly similar dependence of the reflectance on the IOPs: the seawater absorption coefficient, a, and the seawater backscattering coefficient, b_b. The simplest version of this dependence can be expressed in the form (Morel and Prieur, 1977):

$$R_{rs}(\lambda) = const \frac{b_b(\lambda)}{a(\lambda)} \tag{4}$$

The reflectance, not being a seawater IOP, depends also on conditions of the sea surface illumination. It has been shown that seawater reflectance depends rather strongly on the solar zenith angle (SZA) in the case of direct sunlight illumination of the sea surface (Kirk, 1984; Gordon, 1989). However, the total reflectance in the 400-700 nm region only changes from 10 to 15 percent over the entire range of the SZA (Vasilkov and Stephantsev, 1987). This change is small because the increase of the reflectance for direct sunlight illumination with SZA increasing is compensated by reduction of the portion of the direct irradiance in the total irradiance. Changes of spectral ratios of total reflectance are less than about 7 percent over the entire range of the SZA (Vasilkov and Stephantsev, 1987; Morel and Gentili, 1993).

The total IOP is the sum of the IOP of pure seawater and of the three major scattering and absorbing water substances:

$$b_b(\lambda) = b_{bw}(\lambda) + b_{bp}(\lambda) \quad a(\lambda) = a_w(\lambda) + a_{ph}(\lambda) + a_{dom}(\lambda) \tag{5}$$

where subscripts *w, p, ph,* and *dom* denote the pure seawater, the particulate matter, the phytoplankton pigments, and the DOM respectively. The detritus absorption is included in the DOM absorption because of its approximately identical spectral dependence (Carder *et al.,* 1991). The pure seawater absorption coefficient was obtained from Pope and Fry (1997), and from Sogandares and Fry (1997). Values of the pure water absorption coefficient are notably below previous values of Smith and Baker (1981). For Case 2 waters this difference in the pure water absorption coefficient plays a less significant role than for Case 1 waters (Morel, 1996).

The phytoplankton pigment absorption coefficient is normalized through its value at 675 nm:

$$a_{ph}(\lambda) = a_{ph}(675) a_{ph}^*(\lambda) \tag{6}$$

The normalized pigment absorption is given as a hyperbolic tangent function:

$$a_{ph}^*(\lambda) = a_0(\lambda) \exp\{a_1(\lambda) \tanh[a_2(\lambda) \ln(a_{ph}(675) / a_3(\lambda))]\} \tag{7}$$

where the wavelength-dependent parameters $a_i(\lambda)$, $i=0,1,2,3$, are empirically determined. Their values are given in Table 3 (see Subsection 3.3.3) for the cases of "unpackaged" phytoplankton. Equation 7 is different from the chlorophyll-specific absorption parameterization proposed in Bricaud *et al.* (1995). The latter contains only two wavelength-dependent parameters.

The particulate matter backscattering coefficient and the DOM absorption coefficient are accepted in the conventional form:

$$b_{bp}(\lambda) = b_0 (555/\lambda)^n \qquad a_{dom}(\lambda) = a_g(400)\exp[-k(\lambda-400)] \qquad (8)$$

where n is the backscatter wavelength ratio exponent, k is the DOM spectral slope, and $a_g(400)$ is the reference absorption coefficient due to gelbstoff at 400-nm. The DOM spectral slope is set as constant $k=0.0225$ nm^{-1} (Carder, 1999). The Suspended Particulate Matter (SPM) backscatter parameters are empirically related to the remote-sensing reflectance:

$$b_0 = X_0 + X_1 R_{rs}(555) \qquad n = Y_0 + Y_1 \frac{R_{rs}(445)}{R_{rs}(488)} \qquad (9)$$

where X_0, X_1, Y_0, and Y_1 are empirically derived constants listed in Table 3. Their values are adopted from the MODIS processing (part of the SeaDAS software; the small difference in wavelength of the green band at 551 nm instead of 555 nm has been ignored). If the value of n is determined to be negative from Equation 9, it is set to zero.

3.3.2   Inversion Technique

The reflectance model formulated contains three unknowns – $a_{ph}(675)$, $a_g(400)$, and the "constant" term in Equation 4 – provided the remote-sensing reflectance is known from the VIIRS atmospheric correction algorithm. Using spectral ratios of the remote-sensing reflectance eliminates the "constant" term. Two algebraic equations for two unknowns $a_{ph}(675)$ and $a_g(400)$ result from the reflectance ratios:

$$\frac{R_{rs}(412)}{R_{rs}(445)} = \frac{b_b(412)}{b_b(445)}\frac{a(445)}{a(412)} \qquad \frac{R_{rs}(445)}{R_{rs}(555)} = \frac{b_b(445)}{b_b(555)}\frac{a(555)}{a(445)} \qquad (10)$$

The empirical, multi-wavelength algorithms are implemented for $a_{ph}(675)$ and $a_{ph}(400)$ when a value is not returned for the semi-analytical algorithm. The empirical, default algorithms use high $a_{ph}(675)$ and $a_g(400)$ values given by (Carder et al., 2003 and Carder et al., 2004),

$$a_{ph}(675)_{emp} = 0.328 * \left[10^{-0.919+1.037\rho_{25}-0.407\rho_{25}^2-3.531\rho_{35}+1.702\rho_{35}^2} - 0.008\right] \qquad (11)$$

$$a_g(400)_{emp} = 1.5 * \left[10^{-1.147-1.963\rho_{15}-1.01\rho_{15}^2+0.856\rho_{25}+1.579\rho_{25}^2}\right] \qquad (12)$$

where $\rho_{15} = \log[R_{rs}(412)/R_{rs}(555)]$, $\rho_{25} = \log[R_{rs}(445)/R_{rs}(555)]$, $\rho_{35} = \log[R_{rs}(488)/R_{rs}(555)]$.

Chlorophyll a concentration is found from the empirical regression:

$$C = A[\ a_{ph}(675)]^B \tag{13}$$

Values of the coefficients A and B are given in Table 3. If the retrieved value of $a_{ph}(675)$ is greater than $0.03\ \text{m}^{-1}$, an empirical algorithm is used:

$$\log(C) = A_0 + A_1 \log r + A_2 (\log r)^2 + A_3 (\log r)^3 \tag{14}$$

where $r = R_{rs}(488)/ R_{rs}(555)$. Values of empirically derived coefficients are given in Table 3.

To avoid the possibility of a two-mode chlorophyll distribution, there should be a smooth transition in chlorophyll values when the algorithm switches from the semi-analytical to the empirical method. This is achieved by using a weighted average:

$$C = wC_{sa} + (1-w)C_{emp} \tag{15}$$

when the semi-analytical method returns a value of $a_{ph}(675)$ between 0.015 and $0.03\ \text{m}^{-1}$. Here subscripts *sa* and *emp* denote the semi-analytically derived and empirically derived values respectively, and $w = [0.03 - a_{ph}(675)]/0.015$ is the weighting factor.

3.3.3 Empirically Derived Coefficients

Algorithm equations contain a number of empirically derived parameters. Their values are not meant to be universal. They should be updated as more *in situ* measurement data become available. These parameters may also be adjusted for specific regions and seasons to optimize algorithm performance. Parameter values obtained for regions without packaged phytoplankton pigments are given in Tables 3 and 4. The values for regions where packaged and fully-packaged pigments and for the global ocean are given in tables 5-6 as described in more detail in Carder *et al.* (2003) and Carder *et al.* (2004).

Table 3 Wavelength Independent Parameters for Regions Without Packaged Pigments.

X_0	X_1	Y_0	Y_1	A	B	A_0	A_1	A_2	A_3
-1.82E-3	2.058	-1.13	2.57	51.9	1.00	0.2818	-2.783	1.863	-2.387

Table 4 Model Independent Coefficients.

Band	lam	bbw	aw	a1	a2
M1	412	0.003341	0.00480	0.59	-0.48
M2	445	0.002406	0.00742	0.69	-0.48
M3	488	0.001563	0.01632	0.54	-0.48
M4	555	0.000929	0.05910	-0.18	-0.48
M5	672	0.000388	0.43538	0.00	-0.48

Table 5 Model Dependent Coefficients for Phytoplankton Absorption Function a_{ph}.

Model	Global		Unpackaged		Packaged	
Band	a0	a3	a0	a3	a0	a3
M1	1.82	0.014	2.20	0.0112	1.46778	0.017276
M2	3.05	0.014	3.59	0.0112	2.53786	0.017276
M3	1.94	0.014	2.27	0.0112	1.62954	0.017276
M4	0.39	0.014	0.42	0.0112	0.355520	0.017276
M5	1.00	0.014	1.00	0.0112	1.00	0.017276

Table 6 Fully Packaged Model Coefficients for Phytoplankton Absorption Function a_{ph}.

Band	a0	a1	a2	a3
M1	1.019	0.26	-0.45	0.021
M2	1.893	0.45	-0.45	0.021
M3	1.237	0.42	-0.45	0.021
M4	0.316	-0.08	-0.45	0.021
M5	1.000	0.00	-0.45	0.021

3.3.4 Pigment Packaging and Sea Surface Temperature

In deriving the chlorophyll a concentration using the semi-analytical model, the spectrum of $a_{ph}(\lambda)$ is adjusted dynamically using VIIRS-derived SST. Comparing SST in K to the nitrate depletion temperature (NDT) in K, above which nitrate is undetectable (Kamykowski, 1987) as an indicator of nutrient availability provides a space-based cue for evaluating whether upwelling or convective overturn has replenished the surface waters with nutrients from below the surface mixed layer. This changes the species and pigment composition of the phytoplankton assemblage observed, thus requiring adjustments in $a_{ph}(\lambda)$. These phytoplankton are usually small (Herbland et al., 1985) with unpackaged pigments (Carder et al., 1986). The VIIRS SST is used as input (SST and NDT are required to have the same unit) and if the SST is less than NDT−1.0 the pigments are assumed to be fully packaged. If SST is more than NDT+4.0 the pigments are assumed to be unpackaged. Using those end points, anything else may be represented as a weighted average between the two. In order to implement the fully packaged parameters a blending mechanism, identical to that used to transition between the semi-analytic

and empirical algorithm for the unpackaged parameters, is required within the semi-analytic algorithm. The end members in this case are identified as phytoplankton absorption parameters from low-light and nutrient-rich polar waters (packaged) and high-light, nutrient-poor mid-latitude regions. Chlorophyll concentration is calculated using a linear blending algorithm given by,

$$[chla] = w[chla]_{un} + (1-w)[chla]_{fp} \qquad (16)$$

where $[chla]_{un}$ is the unpackaged value, and $[chla]_{fp}$ refers to the fully packaged value. The model branching and weighting factors are given in Table 7. More detail description of the Carder model branching and weighting scheme is given in Carder *et al.* (2003) and Carder *et al*. (2004).

Table 7 Carder Semi-Analytical Model Branching and Weighting for SST vs. NDT

Branching Criteria	Model	pktran	Weight
NDT + 4.0 ≤ SST	Unpackaged	1	1.0
	Unpackaged	1	
NDT + 2.4 ≤ SST < NDT + 4.0	Global	0	(SST – NDT – 2.4) / 1.6
	Unpackaged	1	
NDT + 0.9 ≤ SST < NDT + 2.4	Packaged	2	(SST – NDT – 0.9) / 1.3
	Global	0	
NDT – 1.0 ≤ SST < NDT + 0.9	Fully packaged	3	(SST – NDT + 1.0) / 1.9
	Packaged	2	
SST < NDT – 1.0	Fully packaged	3	1.0
	Fully packaged	3	

3.4 ALGORITHM EVALUATION AND SENSITIVITY STUDIES

3.4.1 Algorithm Evaluation

Evaluation of algorithm performance was conducted using *in situ* measurement data sets. Algorithm error refers to the dispersion in retrieved values of chlorophyll concentration for a given true chlorophyll concentration, in cases where measurement errors in water-leaving reflectance are negligible. This error can be assessed using ship-based measurements of water-leaving reflectance and *in situ* measurements of chlorophyll concentration. Details of this evaluation can be found in Carder *et al.* (2003). Here we present only the main results

concerning root-mean-square (RMS) errors of chlorophyll retrievals. The RMS error is determined by:

$$RMS = \sqrt{\frac{\sum_{i=1}^{N}(C_{\text{mod},i} / C_{obs,i} - 1)^2}{N - 2}}$$
(17)

where subscripts *mod* and *obs* denote modeled and observed values of chlorophyll concentration, and *N* is the number of observations.

For the Carder data subset of the SeaWiFS Bio-Optical Algorithm Mini-Workshop (SeaBAM) evaluation data sets (O'Reilly *et al.*, 1998), the chlorophyll *a* concentrations were predicted with an RMS error of 0.289 (*N*=87). The remote-sensing reflectance was derived from hyperspectral measurements collected just above the sea surface by weighting to simulate SeaWiFS band responses. All chlorophyll *a* values were determined fluorometrically. For a data set with 17 additional high-chlorophyll stations the prediction of chlorophyll concentration was only slightly worse, resulting in RMS of 0.300. The algorithm parameters given in Tables 3 and 4 were used in this evaluation.

The global SeaBAM evaluation data sets (*N*=919) were also used in testing the algorithm. Because many different locations were involved with the global data collection, an attempt was made to partition the data sets into two regions, one where little pigment packaging is to be expected and one where more packaging might be expected. These two subsets will be referred to as "unpackaged" and "packaged." The "unpackaged" data set normally corresponds to high-light, non-upwelling locations in warm, tropical, and subtropical waters. The "packaged" data set was mainly collected in eastern boundary upwelling and high-latitude regions at non-summer times.

For the "unpackaged" data set RMS errors in chlorophyll concentration were 0.242 (*N*=287). The algorithm parameters used were the same as in Tables 3 and 4. For the "packaged" data the algorithm parameters $a_i(\lambda)$, *A, B*, and A_i were slightly changed. The RMS error of 0.282 was obtained for this data set (*N*=326).

A "global" average algorithm was also developed for use at times and places where pigment packaging is unknown or transitional. It was tested on a global data set combining the "packaged," "unpackaged," and other mixed data sets from SeaBAM. A set of compromise parameters has been developed for the global algorithm. The algorithm predicted chlorophyll concentration with the RMS error of 0.440 (*N*=976).

A comparison of the algorithm with the SeaWiFS algorithm (Equation 2) is given in Figures 1 and 2. The Carder algorithm was parameterized for global application.
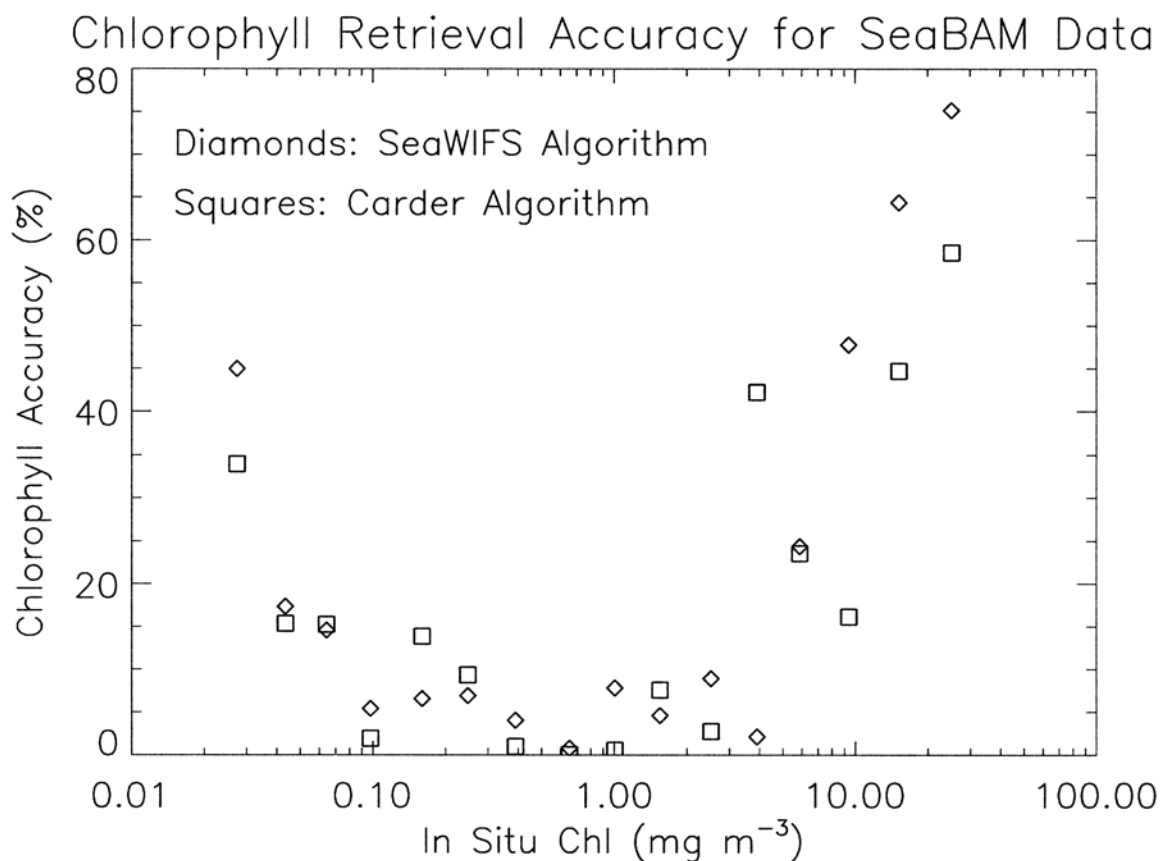
Figure 1. Comparison of the accuracy of chlorophyll retrievals from the Carder algorithm with the accuracy of chlorophyll retrievals from the SeaWiFS algorithm.

Both algorithms were applied to remote sensing reflectances from the SeaBAM data set, and accuracy and precision were calculated within 16 bins of log (*in situ* chlorophyll concentration) over the range $-1.7 \leq$ log (*in situ Chl*) ≤ 1.5. This corresponds to $0.02 \leq$ *in situ Chl* ≤ 32 mg m^{-3} and includes nearly all of the SeaBAM data. The Carder algorithm gives better accuracy than the OC2v2 algorithm for 11 of the bins and worse accuracy for 5 of the bins. On average, the Carder algorithm accuracy values are 3.1% better than the OC2v2 algorithm accuracy values. A more important point is that the Carder algorithm accuracy is better for low and high chlorophyll concentrations. Currently, the SeaWiFS algorithm meets the uncertainty requirement of ±35% only within a range of 0.05<*Chl*<1 mg/m^3(Aiken et al., 1998). The Carder algorithm accuracy is better beyond this range. It should be noted that evaluation of the performance of ocean color sensors is not simple. For example, less than 5 percent of *in situ* data collected for verification of the SeaWiFS products in different research vessel cruises could meet quality control criteria and be used for comparison (McClain *et al.*, 1998).
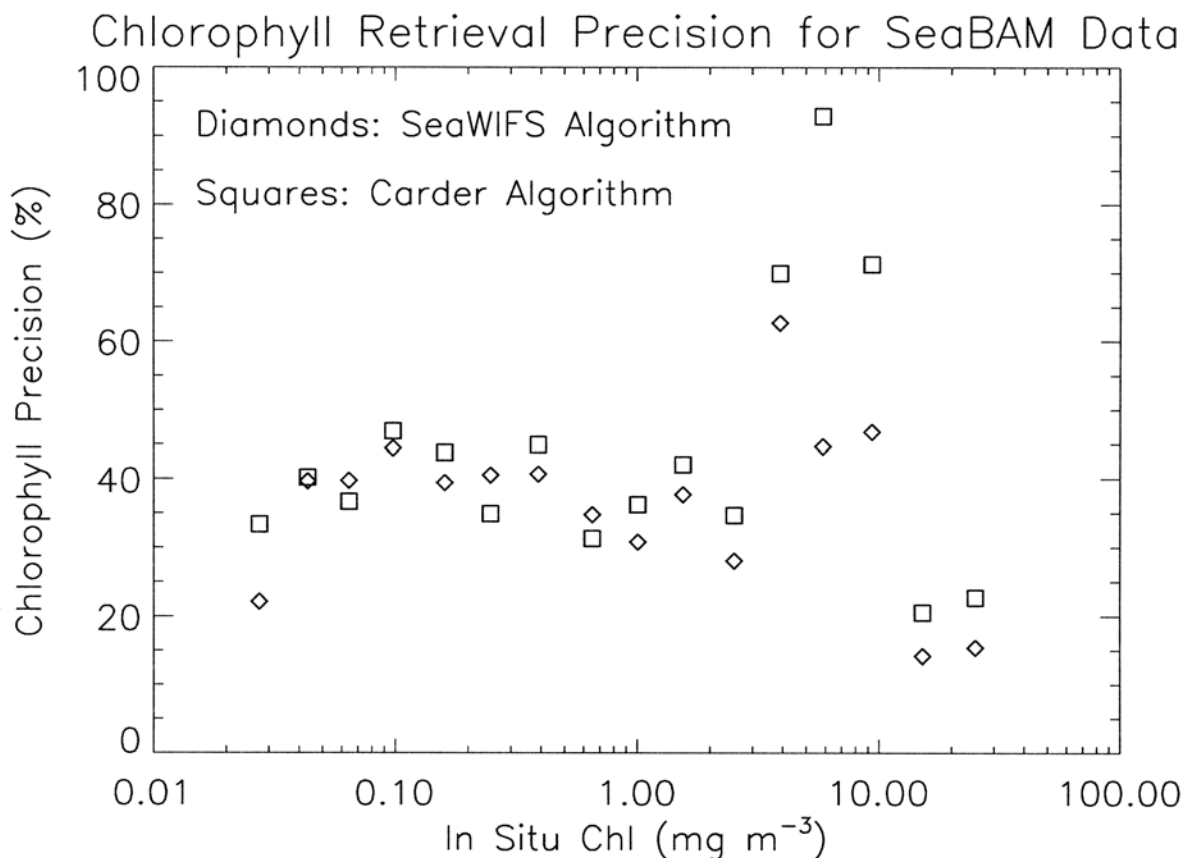
Figure 2. Comparison of the precision of chlorophyll retrievals from the Carder algorithm with the precision of chlorophyll retrievals from the SeaWiFS algorithm.

The Carder algorithm gives better precision than the OC2v2 algorithm for 3 of the bins and worse precision for 13 of the bins. On average, the Carder algorithm precision values are 7.5% worse than the OC2v2 algorithm precision values. Although the Carder algorithm precision is slightly worse than the SeaWiFS algorithm, the Carder algorithm precision can be improved potentially by specifying regional values of the pigment packaging parameter. In the future this could be accomplished by using VIIRS SST data (Carder *et al.*, 1999).

Currently, algorithm error is typically on the order of 50 percent for global application of most bio-optical algorithms (e.g., O'Reilly *et al.*, 1998). However, tuning of algorithms can result in algorithm error as low as 20 percent for specific regions. For example, a comparison shown in Figure 3 of retrieved and *in situ* chlorophyll for a region in the equatorial Pacific results in RMS error of 18.1 percent. *In situ* chlorophyll and water-leaving reflectance were measured by C. Davis on two cruises in the region in spring and fall of 1992, and the retrieved values are from the Carder algorithm parameterized for unpackaged pigments.

A bio-optical algorithm error of 18% was estimated by using *in situ* measured reflectance and chlorophyll data. The *in situ* data already bears the error of instruments used in shipboard measurements of seawater reflectance and chlorophyll concentration. This kind of error should

be excluded while estimating the bio-optical algorithm error itself. Unfortunately, the measurement errors are not well known. They are not reported along with data used in bio-optical algorithm error estimations. This bio-optical algorithm error of 18% gives the upper estimate of inherent algorithm error.

The inherent chlorophyll algorithm error should include an uncertainty of chlorophyll retrievals, which is due to the natural variability of optically active constituents not accounted for by the chlorophyll algorithm. Reflectance and chlorophyll measurements are assumed to be ideal with no error at all. The natural variability may include pigment species variability, pigment packaging effects, variability of DOM absorption spectral slope, SPM concentration variability, and SPM spectral backscatter variability. Bi-directional effects of the seawater reflectance also contribute to natural variability uncertainty.

Theoretical estimates of the bio-optical algorithm error were achieved by simulations of chlorophyll retrievals from the reflectance model (Morel, 1988) with perturbations introduced in inherent optical properties (IOPs). Perturbations were determined from uncertainties of the reported empirical data (Bricaud *et al.*, 1981). The spectrally correlated perturbations of IOPs modeled natural variability of optical properties. Depending on the type of spectral behavior of perturbations, the Carder algorithm error was 6-9% in the best case and 13-18% in the worst case. Hence, the bio-optical algorithm error of 10% was adopted as the lower estimate of the inherent algorithm error. To illustrate difficulties in estimating the algorithm inherent errors from reflectance and chlorophyll measurements, spectral reflectance measured for a narrow bin of chlorophyll concentration is shown in Figure 4, the data for which were taken from SeaBAM data sets. It is clear that band radiance ratios, which the algorithm uses, vary significantly while the chlorophyll concentration is almost constant.

The theoretical estimate of the random bio-optical algorithm error is valid for Case 1 waters only. For Case 2 waters with chlorophyll concentration greater than about 2-3 mg/m^3, the empirical estimate of the random bio-optical algorithm error is currently used in the chlorophyll error budget. The precision of the chlorophyll retrievals from the Carder algorithm parameterized for global application was estimated by using remote sensing reflectances and chlorophyll concentrations from the SeaBAM datasets (O'Reilly et al., 1998). Because the SeaBAM datasets lack information for high chlorophyll concentrations, the chlorophyll precision was determined by averaging all available chlorophyll concentrations greater than 3 mg/m^3. The resulting algorithm precision is about 30%. This estimate gives the upper limit of the algorithm random error for Case 2 waters. Hence, a bio-optical algorithm random error of 20% representing the mean error was adopted. This best estimate accounts for possible future improvement to the Carder algorithm performance, for example, by the regional adjustment of the pigment packaging parameter used by the algorithm.

The systematic chlorophyll algorithm error is caused by approximations made in the remote sensing reflectance model and parameterization of the IOPs. An estimate of the systematic algorithm error was done by comparison of *in situ* measured and retrieved chlorophyll concentrations. The accuracy of the chlorophyll retrievals from the Carder algorithm parameterized for global application was estimated by using remote sensing reflectances and chlorophyll concentrations from the SeaBAM dataset (O'Reilly et al., 1998). The chlorophyll accuracy strongly depends on the chlorophyll concentration. Therefore, the algorithm systematic

error was stratified over the chlorophyll measurement range. The following best estimates of the systematic algorithm error were adopted. The error is equal to 15% for chlorophyll concentrations Chl < 0.1 mg m^{-3}, 10% for $0.1 \leq$ Chl ≤ 1.0 mg m^{-3}, 20% for $1.0 <$ Chl ≤ 10.0 mg m^{-3}, and 30% for Chl > 10 mg m^{-3}. These estimates of the algorithm systematic error were used in the chlorophyll error budgets.
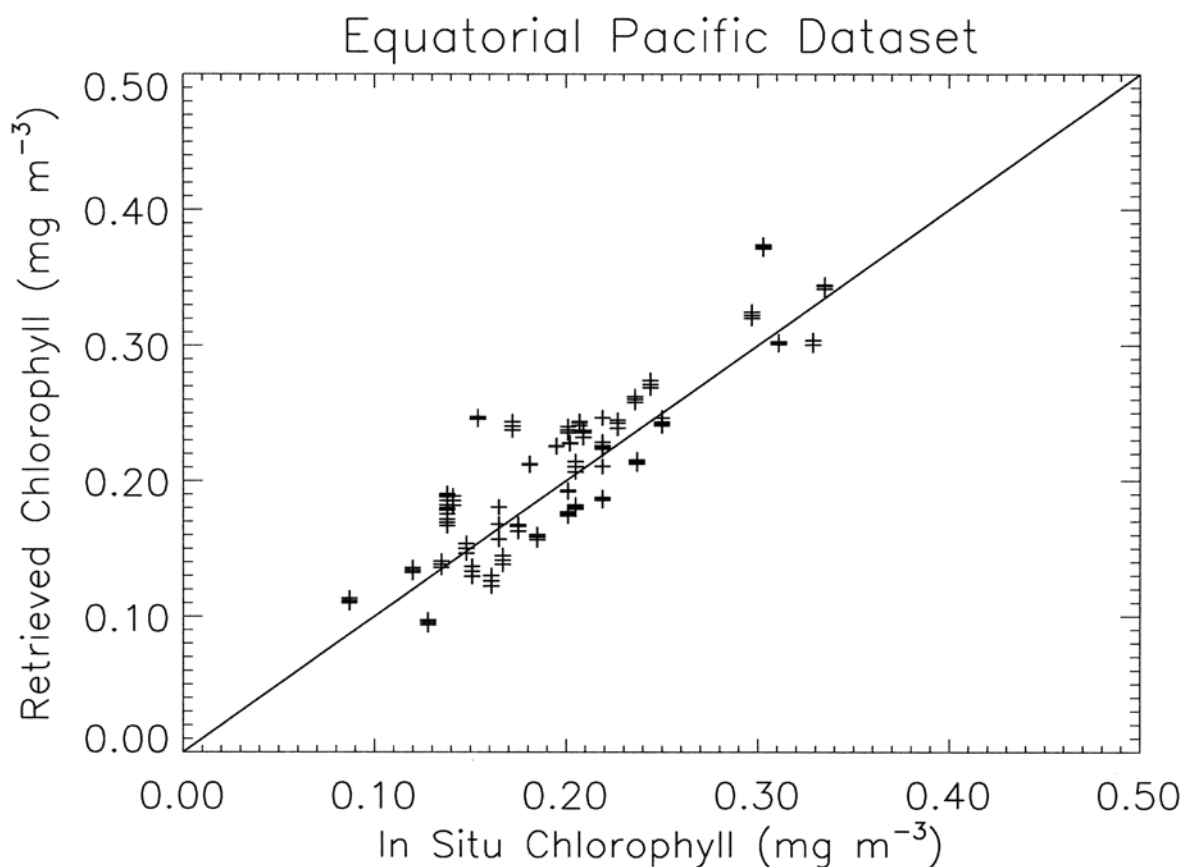

Figure 3. **Comparison of chlorophyll contracation retrievals with in-situ data from the equatorial Pacific subset.**

3.4.2 Sensor Noise Sensitivity Study

Algorithm sensitivity to sensor radiometric noise was studied using simulated reflectance spectra. Top-of-atmosphere (TOA) radiances over the ocean were simulated at 412, 445, 488, and 555 nm using the 6S code of Vermote *et al.* (1997). This code uses the reflectance model for Case 1 waters (Morel, 1988) to simulate water-leaving radiance for a given chlorophyll concentration and performs forward transfer to the top of the atmosphere. The simulations were conducted for March 21, and standard atmospheric parameters used for the simulations are water vapor content 0.85 g/cm^2, ozone content 0.395 cm atm, aerosol type maritime, visibility 23 km, and wind speed 5 m/s. Simulations were calculated over a grid covering the VIIRS orbit swath from −75 to +75 degrees latitude and from −54 to +54 degrees sensor zenith angle (corresponding to a swath width of 2400 km), for the 9:30 am orbit or the 1:30 pm orbit.

Use of the Morel 1988 reflectance model was chosen after comparison of the predictions of three reflectance models with ship-based measurements from the SeaBAM data set. The comparison is shown in Figure 4. The triangles in the figure show SeaBAM measurements of the remotely sensed water-leaving reflectance as a function of wavelength for positions where *in situ* measurements of chlorophyll concentration were within 2 percent of 0.1 mg/m^3, a value typical
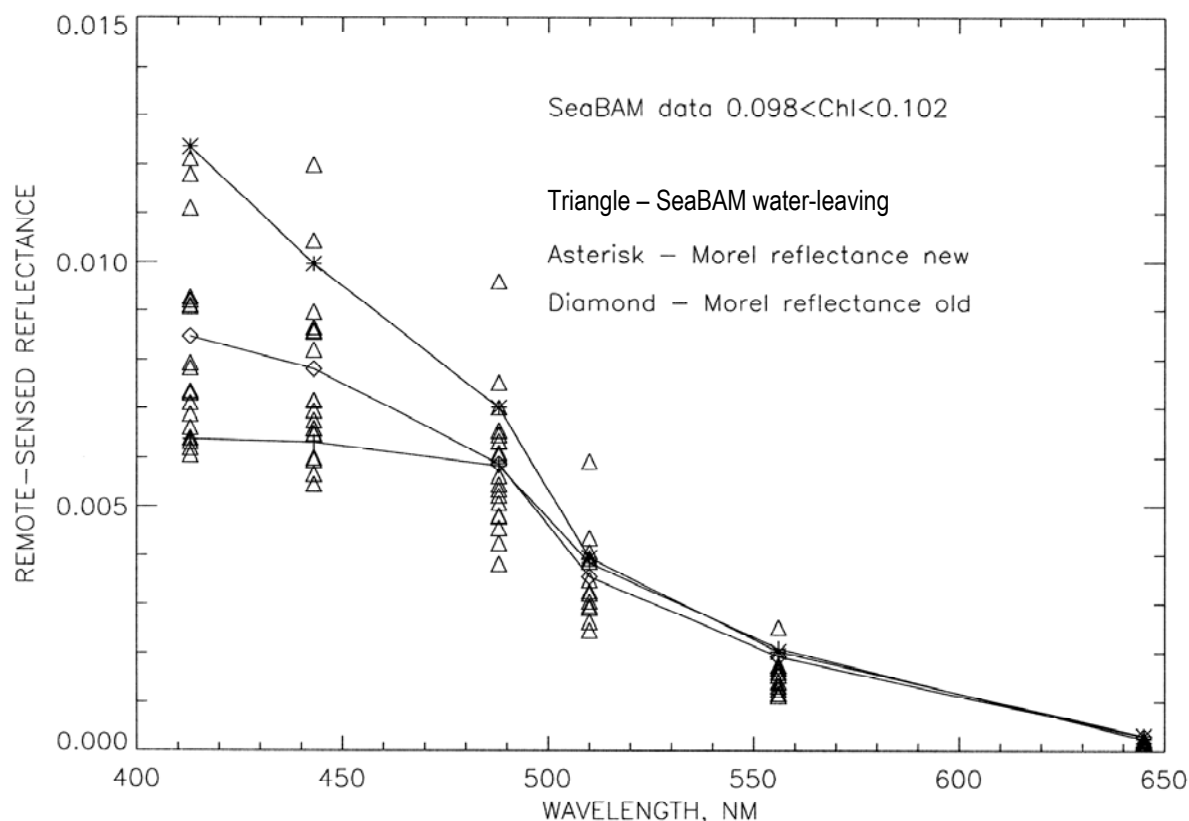

Figure 4. Remote-sensing reflectance spectra of the SeaBAM data sets, for *in situ* chlorophyll concentration between 0.098 and 0.102 mg m^{-3}, compared with different reflectance models.

for the open ocean. Predicted water-leaving reflectances for this chlorophyll concentration are shown as diamonds for the Morel 1988 model, as asterisks for a new version of the Morel model that includes the most recent pure water absorption coefficients (Pope and Fry, 1997; Sogandares and Fry, 1997). The figure shows that the Morel 1988 model provides the most realistic prediction of water-leaving reflectance at low chlorophyll concentrations. The Carder retrieval algorithm for unpackaged pigments is more appropriate for gelbstoff-rich subtropical waters of outer continental shelves than for the global waters in the SeaBAM data set. An inverse of the Carder retrieval algorithm parameterized for global waters predicts water-leaving reflectances that are in better agreement with the SeaBAM measurements; this model may be adoped for use in our future simulations.

Sensor noise was added to the simulated TOA radiances for each of the seven VIIRS sensor performance models described in Hucks (1998). The sensor model 1 has an "effective aperture diameter" of 29 cm. Each subsequent sensor model has the effective aperture diameter of 5 cm

less. All other sensor parameters are fixed for the sensor models. However, the sensor noise models do not necessarily imply those aperture sizes. Noise-equivalent delta radiance (NEdN) was calculated following Hucks (1998). NEdN values calculated for a single VIIRS pixel were reduced by the square root of the number of pixels aggregated to meet the horizontal cell size requirement for chlorophyll. Sensor model 0 is the noise free case simulated to provide quality statistics in the absence of sensor noise.

NEdN was calculated for each band and for each viewing geometry used in the TOA radiance simulation. Two methods were used for the addition of sensor noise and the subsequent determination of chlorophyll precision. In one method, 100 different random samples of the Gaussian noise distribution were obtained for each band and for each viewing geometry in a grid of 7 sensor zenith angles x 16 latitudes covering the viewing swath. This provided 100 different maps on this grid of noise-added simulated radiance in each band. Retrieval was performed to obtain 100 different chlorophyll maps, and chlorophyll precision at each position was calculated as the standard deviation of the 100 chlorophyll values divided by the mean of the chlorophyll values. In the other method, the noise distribution was sampled only once at each position in a much finer grid covering the swath, giving one map of noise-added simulated radiance in each band. The mean chlorophyll precision over the swath was calculated as the standard deviation of all retrieved chlorophyll values divided by the mean of all retrieved values.

Retrieval of chlorophyll concentration from TOA radiances is performed in two steps. Atmospheric correction is performed to obtain water-leaving reflectances in the visible bands, and a bio-optical algorithm is then used to retrieve chlorophyll concentration from the water-leaving reflectances.

Table 5 lists values of chlorophyll precision due to sensor noise in the visible bands, averaged over the 1:30 PM or 9:30 AM viewing swath, for a series of 13 different simulations.

Table 6 Chlorophyll Precision (%) Due to Sensor Noise

Sensor Model	Simulation Number												
	1	2	3	4	5	6	7	8	9	10	11	12	13
1	7.4	11.8	16.0	10.0	8.7	9.9	10.0	7.2	5.0	5.1	8.2	2.2	3.5
2	9.9	17.0	19.3	13.2	11.6	13.7	13.9	9.6	6.4	6.0	10.3	2.7	4.5
3	11.5	20.0	26.7	15.2	13.0	16.0	15.2	11.2	7.2	7.6	13.2	3.2	5.6
4	16.0	26.2	40.3	20.5	18.1	21.3	22.9	15.5	9.7	10.2	18.6	4.7	7.8
5	30.5	38.6	138	42.0	29.8	50.3	61.5	30.1	16.9	20.9	33.3	9.2	15.1
6	408	910	717	818	**	441	698	351	155	112	**	28.2	**

The ** indicates a value greater than 1000. Simulation 1 is a nominal simulation for chlorophyll concentration of 0.1 mg/m^3 using the Morel 1988 model for water-leaving reflectance, atmospheric visibility of 23 km, aggregation to 1.3 km cell size, and baseline bandwidths of 15, 20, 10, and 21 nm at wavelengths 412, 445, 488, and 555 nm, respectively. Mean chlorophyll precision for simulation 1 was calculated over a 1:30 pm orbit swath of width 2400 km at positions where the solar zenith angle is less than 70 degrees. The other simulations are variations on Simulation 1, as shown in Table 7.

Table 7 Variations on Simulation 1

Simulation Number	Difference(s) From Simulation 1
2	Chl = 1.0 mg/m3
3	Chl = 5.0 mg/m3
4	Visibility 5 km
5	9:30 am orbit
6	Carder water-leaving reflectance model
7	All bandwidths 20 nm
8	1800 km swath width
9	Chl = 1.0 mg/m3, 1800 km swath width
10	2.6 km cellsize
11	Chl = 1.0 mg/m3, 2.6 km cellsize

Figure 5 shows how the precision due to visible band sensor noise varies over the 1:30 PM orbit swath for Simulation 1. Figures 6 through 8 show comparisons of mean precision from different simulations as a function of sensor performance model.
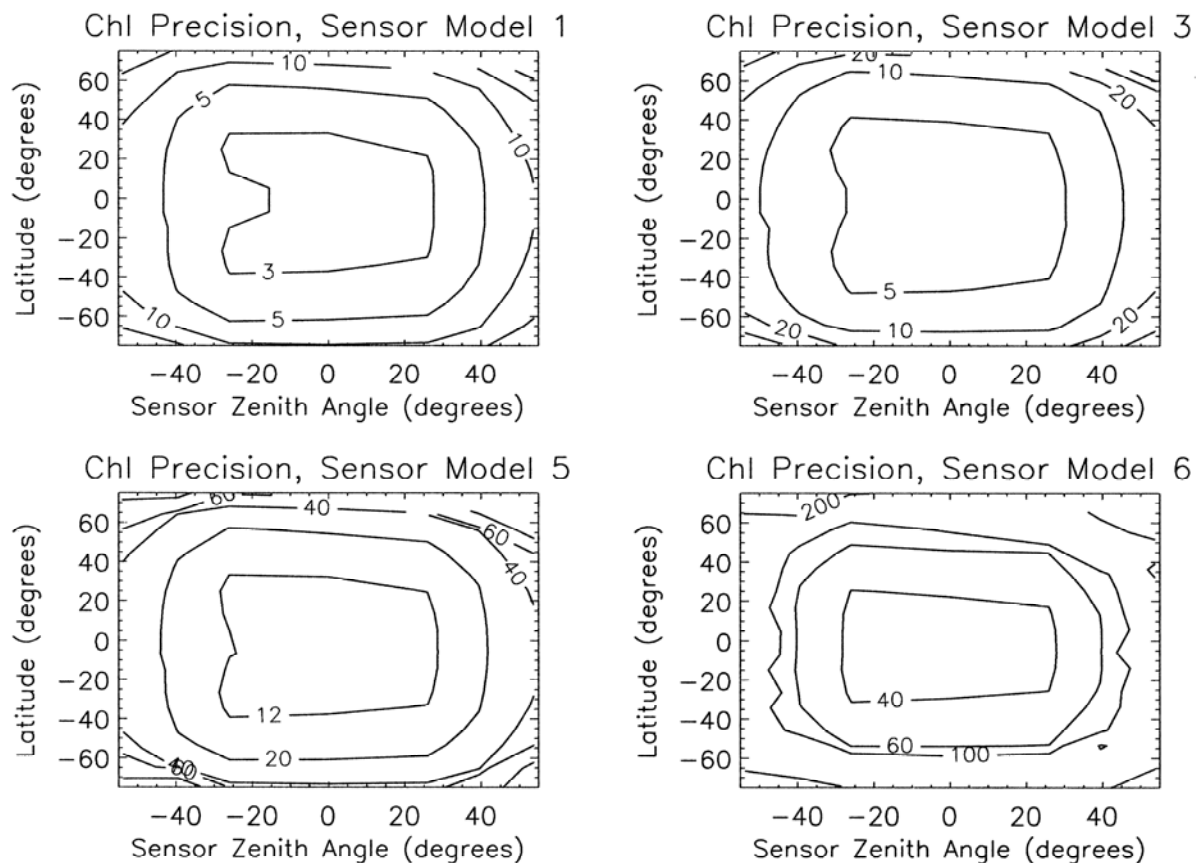
Figure 5. Contour maps of chlorophyll precision due to sensor noise in the visible bands over the viewing swath of the 1:30 pm orbit for Simulation 1. The contour labels give precision in percent. The full range of sensor zenith angle shown corresponds to a swath width of 2400 km. The threshold value for minimum swath width for chlorophyll is 1700 km (TBR), which corresponds to a range of -37 to +37 degrees in viewing zenith angle of the sensor.
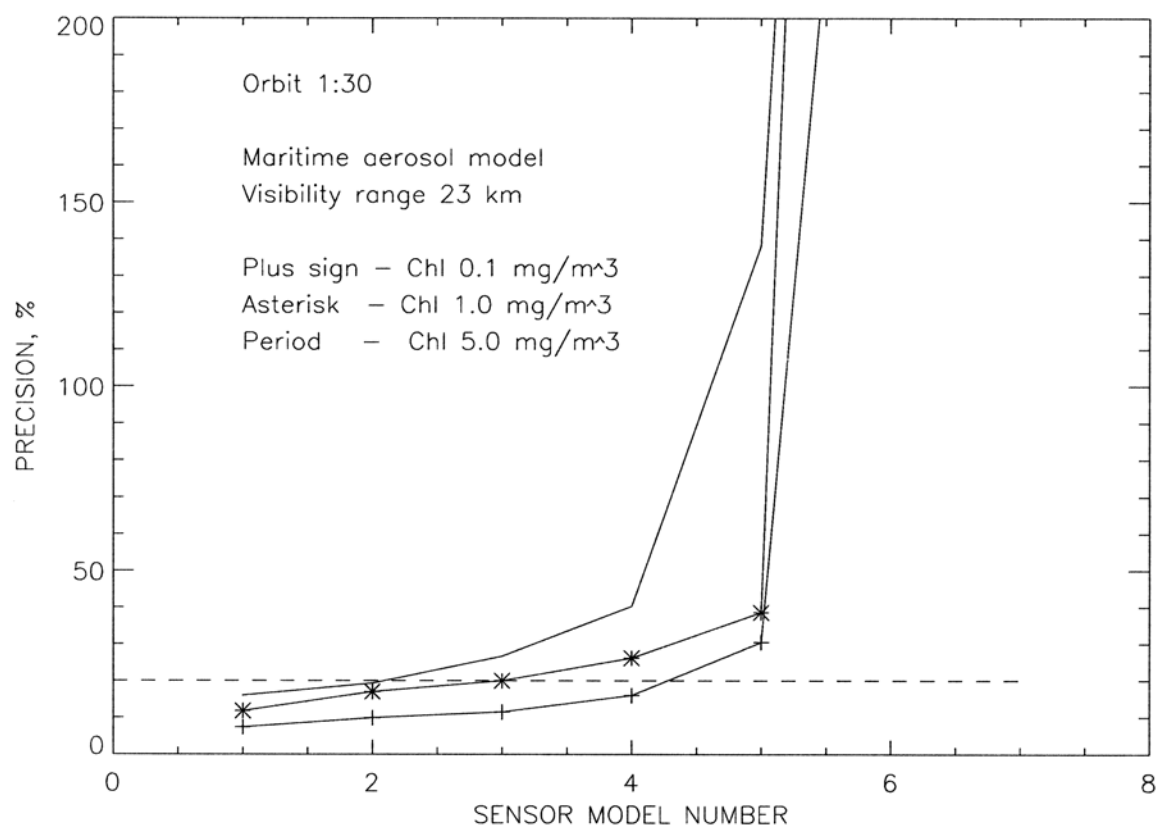
Figure 6. Mean chlorophyll precision due to noise in visible bands as a function of sensor performance model, for different chlorophyll concentrations (simulations 1-3). Dashed line is the system requirement in precision.
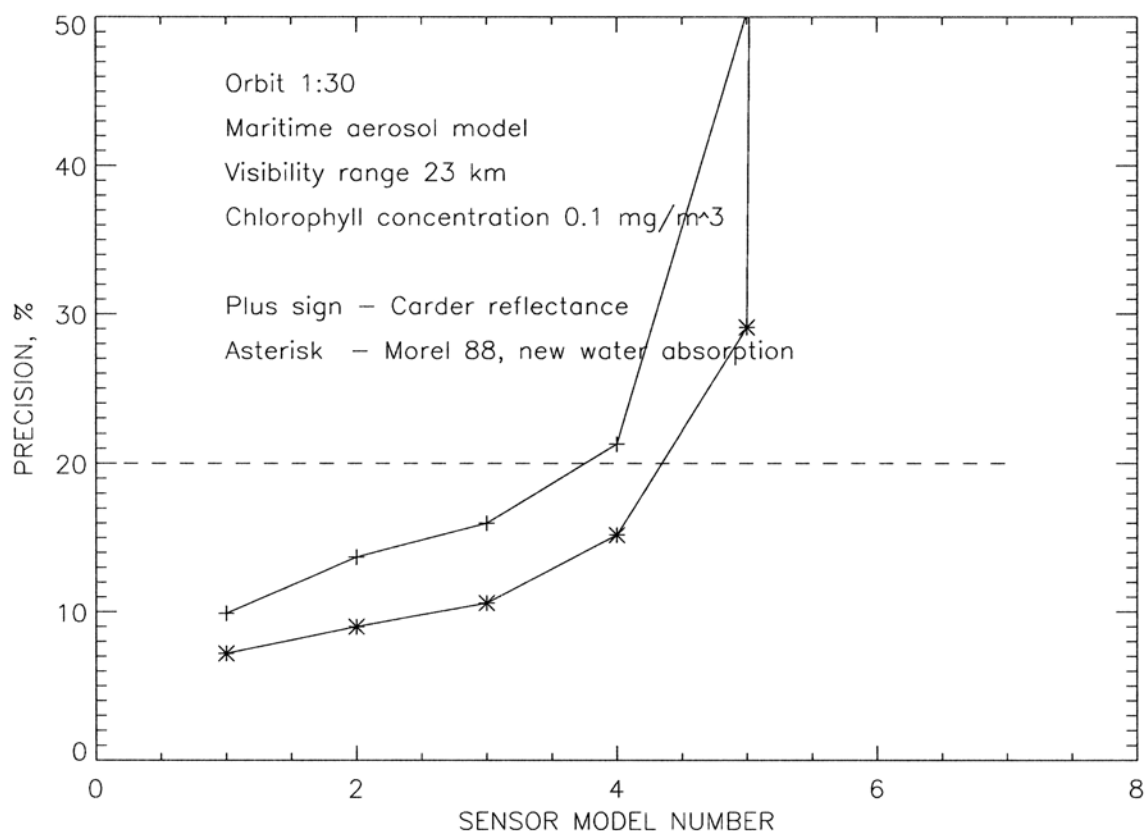
Figure 7. Comparison of mean precision due to visible band sensor noise when different water-leaving reflectance models are used in the simulation. The Carder reflectance model results in poorer precision because it gives lower water-leaving reflectance (and hence lower signal-to-noise ratio) in the blue bands (see Figure 2). Dashed line is the system requirement in precision.
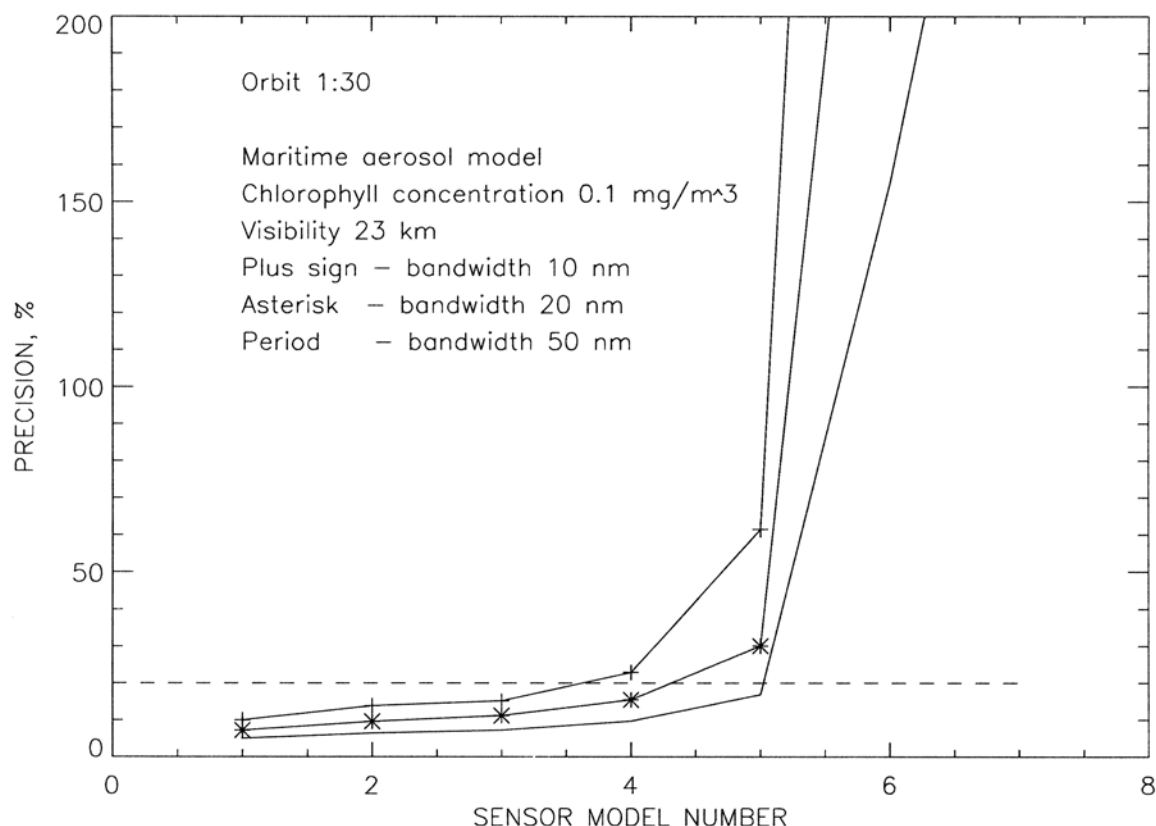
Figure 8. Dependence of mean precision due to visible band sensor noise on bandwidth of visible bands, for chl = 0.1 mg/m^3 (simulations 7-9). Dashed line is the system requirement in precision.

3.4.3 Sensitivity Study Conclusions

During phase I, VIIRS sensor performance model 3 was recommended as sufficient to meet the chlorophyll precision requirement of 20 percent, at least for typical open ocean chlorophyll concentrations and atmospheric conditions. Much iteration of sensor specifications occurred subsequent to this recommendation but the minimum requirement has been maintained with additional engineering margin applied. Please see sensor specification for presently specified SNR values. Table 8 lists values of precision averaged over a bin at the edge of the 1:30 pm orbit swath, where in-scan position is between 600 and 900 km and solar zenith angle is less than 70 degrees. (A minimum swath width of 1,700 km has been specified for VIIRS chlorophyll retrievals because sensors in 9:30 am and 1:30 pm orbits provide nearly complete global coverage in 48 hours for a swath width of 1,700 km. 48 hours is the threshold for maximum local average revisit time.) Results are shown for chlorophyll concentration values of 0.1, 1, and 5 mg m^{-3} (Simulations 1-3 described above). Precision values listed were calculated as the square root of the sum of the squares of chlorophyll precision due to sensor noise and chlorophyll precision due to algorithm error. A value of 18 percent was adopted for the precision due to algorithm error in all cases. Table 9 lists the fraction of the bin area for which the chlorophyll precision is better than 20 percent, for the same simulations.

Table 8. Mean Chlorophyll Precision (%) for 1:30 pm Orbit

Chlorophyll (mg m-3)	Sensor Model 0	Sensor Model 1	Sensor Model 2	Sensor Model 3	Sensor Model 4	Sensor Model 5
0.1	18.0	19.1	19.7	20.3	22.4	32.7
1.0	18.0	22.0	23.3	24.9	29.4	48.1
5.0	18.0	23.8	26.6	36.9	42.0	95.1

Table 9 Fraction of Area Meeting the 20% Precision Threshold for 1:30 pm orbit

Chlorophyll(mg m^{-3})	Sensor Model 0	Sensor Model 1	Sensor Model 2	Sensor Model 3	Sensor Model 4	Sensor Model 5
0.1	1.00	0.88	0.81	0.73	0.35	0.00
1.0	1.00	0.46	0.35	0.27	0.00	0.00
5.0	1.00	0.42	0.23	0.08	0.00	0.00

Meeting the 20 percent precision threshold is much more difficult for coastal regions than for the open ocean, because the chlorophyll concentration is larger (values typically 1.0 mg/m^3 and higher, compared to a typical open ocean value of about 0.2 mg/m^3). The results given in Tables 8 and 9 are for a cell size of 1.3 km.

The algorithm error component of 18 percent is generally the largest contributor to the error budget for the better sensor models, and this is the most difficult of the components to assess because it requires predicting algorithm performance for NPOESS constellation completion. Table 10 provides precision results calculated as above but without including the algorithm error.

Table 10 Mean Chlorophyll Precision due to Sensor Noise (%) for 1:30 pm orbit

Chlorophyll (mg m^{-3})	Sensor Model 0	Sensor Model 1	Sensor Model 2	Sensor Model 3	Sensor Model 4	Sensor Model 5
0.1	0.0	5.8	7.2	8.6	12.3	25.7
1.0	0.0	11.5	13.6	16.1	22.3	43.4
5.0	0.0	13.8	17.8	29.4	35.9	92.1

The global frequency distribution of a given chlorophyll concentration can be provided by using biological classification of ocean waters. All ocean waters are roughly divided into three categories: oligotrophic waters with chlorophyll $Chl < 0.1$ mg/m^3, mesotrophic waters with chlorophyll 0.1 mg/m^3 $< Chl < 1.0$ and eutrophic waters with chlorophyll $Chl > 1.0$ mg/m^3. According to CZSC-derived global chlorophyll statistics (Antoine *et al*., 1996), oligotrophic waters comprise 55.8% of the ocean area, mesotrophic waters comprise 41.8% of the ocean area, eutrophic waters comprise 2.4% of the ocean area. These numbers give an insight into the frequency of specific chlorophyll concentrations on global scale.

A comparison of the precision at nadir and at the edge of scan is given in Figure 9 for different chlorophyll concentration (bio-optical algorithm error of 10% was adopted in these simulations).
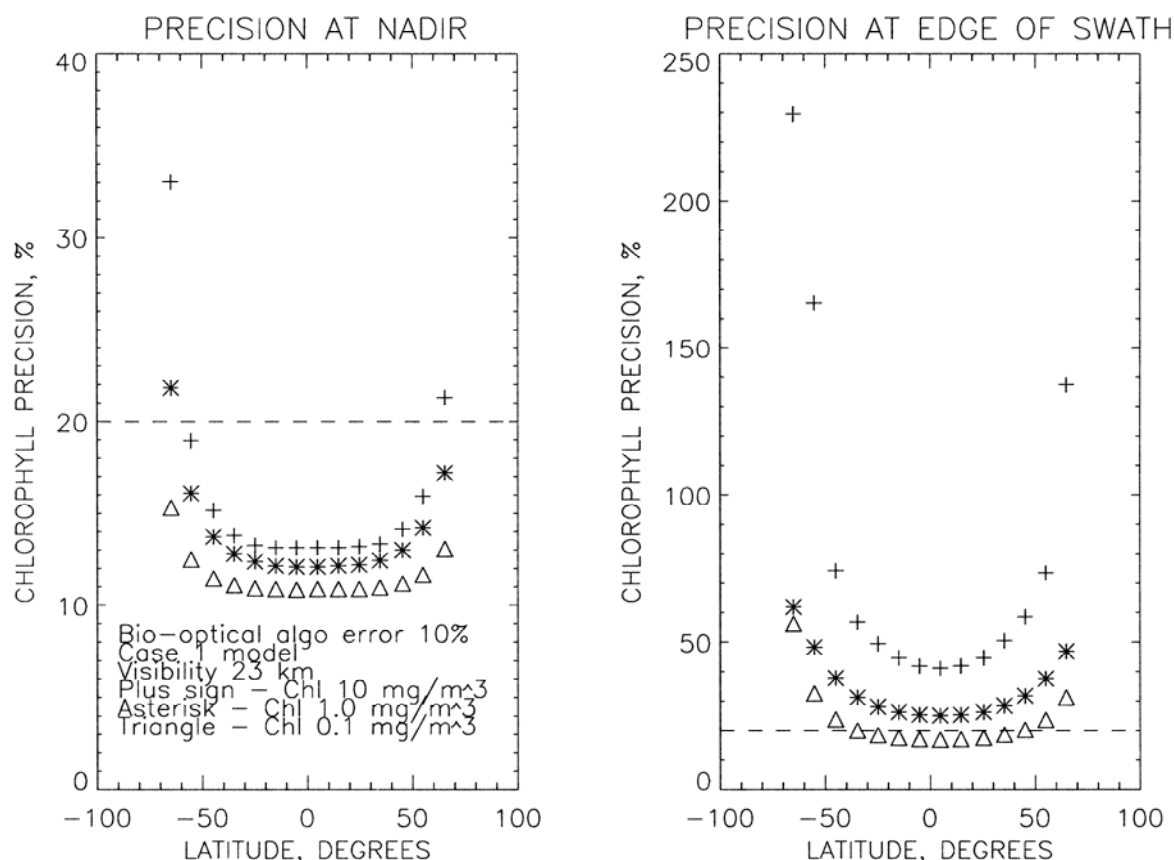

Figure 9. Comparison of the chlorophyll precision at nadir and at the edge of scan.

Figure 9 shows that the chlorophyll precision at nadir is considerably better than at the edge of scan, under the conditions described above. To improve the chlorophyll precision at the edge of scan a statistical approach can be used for overlapping data measured by two satellites for two days. The best viewing geometry values for two sensors measuring for two days is an alternative.

Overall performance of the Carder algorithm was also evaluated on a global scale. A SeaWiFS monthly map of chlorophyll concentration was used as input for calculating water-leaving radiance by using the Case 1 water reflectance model (Morel, 1988). To avoid inconsistency between the reflectance model and the retrieving algorithm, the chlorophyll concentrations were first retrieved from calculated remote-sensing reflectance by using the Carder algorithm and those chlorophyll concentrations were considered as true. TOA radiances were calculated by using forward modeling with the exact matrix method of radiative transfer in the atmosphere. Gaussian radiometric noise corresponding to baseline and spectrally correlated sensor calibration error of 0.5% were added to the TOA radiances. Atmospheric correction of the error-added TOA radiances was performed to retrieve the remote sensing reflectance in the visible bands. The Carder bio-optical algorithm was applied to the remote sensing reflectance to retrieve the

chlorophyll concentration. The retrieved chlorophyll concentrations were compared to the true concentrations for each pixel.

To estimate the chlorophyll accuracy and precision, a range of true chlorophyll concentrations in the logarithmic scale was divided into 10 equal bins. For each bin mean values of the true chlorophyll concentration, μ_T, and the retrieved chlorophyll concentration, μ, were calculated. The chlorophyll accuracy for each bin was determined as:

$$A = |\mu - \mu_T| / \mu_T \tag{18}$$

and the chlorophyll precision was calculated as:

$$P = \frac{\sqrt{\sum_{i=1}^{N} [C_{Ri} - C_{Ti} - (\mu - \mu_T)]^2 / (N-1)}}{\mu_T} \tag{19}$$

where C_R is the retrieved concentration for given pixel, C_T is the true concentration, and N is the number of retrievals for the bin. The above definition of the chlorophyll precision (suggested in Miller, 1998) accounts for variance of true values within the bin. In other words, precision corresponds to the bias-adjusted RMS for situations with variable truth. The chlorophyll accuracy and precision are shown in Figure 10 as a function of the true chlorophyll concentration. Relative chlorophyll concentration frequency is also shown in Figure 10. As it can be seen from Figure 10 the algorithm performance is quite good except for high chlorophyll concentrations.
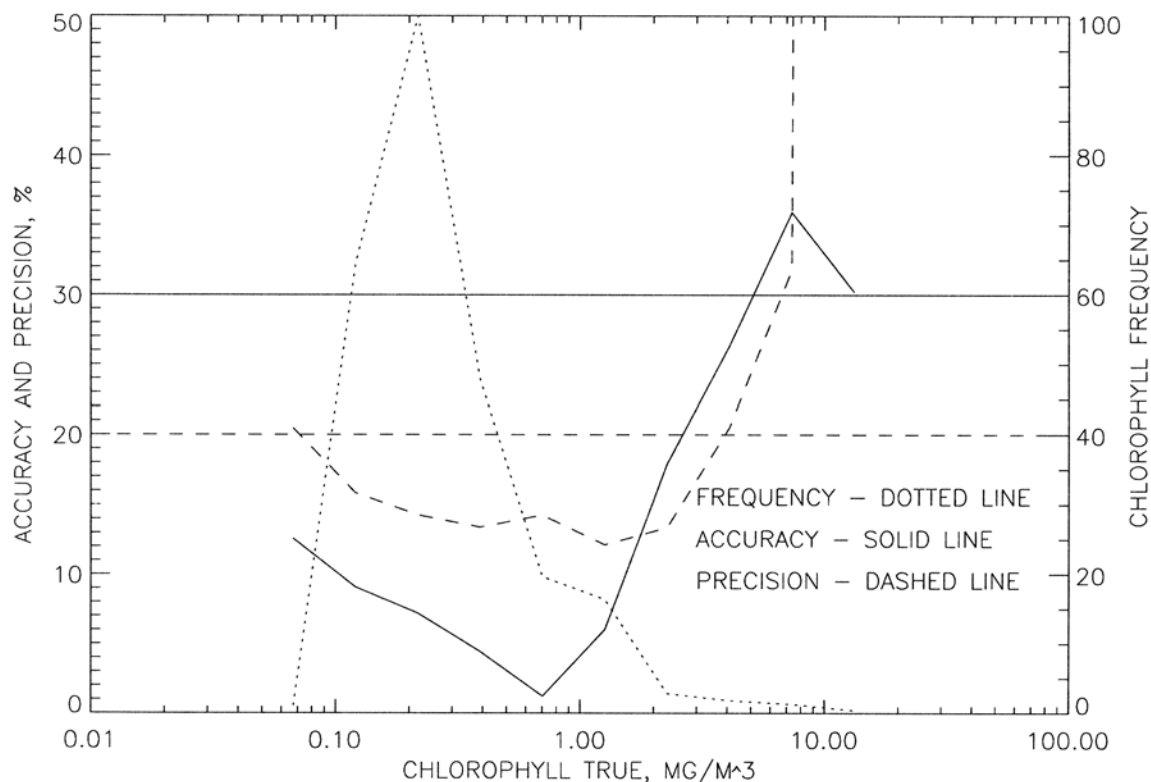
Figure 10. Global chlorophyll accuracy and precision as a function of true chlorophyll concentration.

3.4.4. Sensor Specification and Predicted Performance

Final simulations were done for radiometric noise corresponding to sensor specification and predicted performance. A general scheme of the simulations is shown in Figure 11. For a given chlorophyll concentration, the remote sensing reflectance was calculated using reflectance models for Case 1 and Case 2 waters. For Case 1 waters, the well-known reflectance model suggested by Morel (1988) was used. For Case 2 waters, a reflectance model based on empirical regressions (Tassan, 1994) was used (Vasilkov, 1997). According to this model, suspended particulate matter (SPM) concentration is higher for a given chlorophyll concentration than for the Case 1 reflectance model. The model can be referred to as a sediment-rich reflectance model.

TOA radiances were calculated using the adapted two-layer model after Gordon and Wang (1994) and a radiative transfer code by Liu and Rupert (1996). A maritime aerosol model with humidity of 80% was used in simulations of the TOA radiances. This aerosol model having humidity of 80% was not included in candidate models of the atmospheric correction algorithm. Most simulations were done for a baseline visibility range of 23 km corresponding to aerosol optical thickness of 0.15 at wavelength of 550 nm. Simulation geometries correspond to the 13:30 satellite orbit.

The TOA radiances were perturbed by Gaussian radiometric noise representing both sensor specification and predicted performance *[# PS154640-101A]*. A spectrally correlated calibration

error of 0.5% was added to the TOA radiances. The value of the calibration error is believed to be reasonable for the post-launch vicarious calibration of the sensor and algorithms (Gordon, 1997). The TOA radiances were also perturbed by a whitecap reflectance error corresponding to an uncertainty in wind speed of 1 m/s at a nominal value of wind speed of 6 m/s. Sensor polarization sensitivity was assumed to be equal to 3% in all visible and NIR bands with an uncertainty of 0.5%.
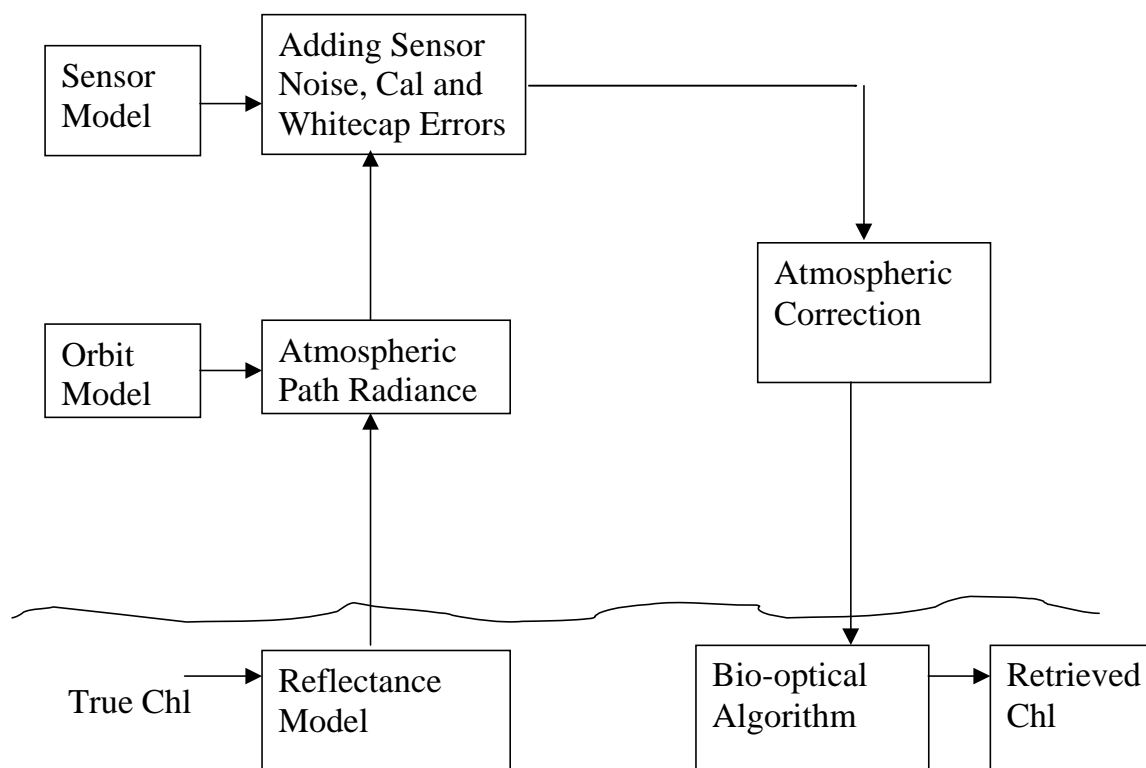

Figure 11. Shows a general scheme of simulations carried out to estimate the chlorophyll accuracy and precision for sensor specification and predicted performance.

Atmospheric correction was applied to the perturbed TOA radiances to retrieve remote sensing reflectances. The atmospheric correction algorithm (Gordon and Wang, 1994) was modified to include sensor polarization sensitivity correction. More details can be found in the Atmospheric Correction over the Ocean ATBD (SRBS Document # Y2411, version 5, 2002). Chlorophyll concentrations were retrieved from the remote sensing reflectances using the Carder bio-optical algorithm. Retrieved chlorophyll concentrations were compared to the true chlorophyll concentrations and chlorophyll precision and accuracy were calculated. The chlorophyll precision significantly depends on both the solar zenith angle (SZA) and viewing geometry. Therefore, the chlorophyll precision was calculated at nadir and edge of swath (EOS) by averaging over SZA of the satellite orbit. The chlorophyll accuracy appeared to be almost independent of viewing geometry.

The chlorophyll precision for the EDR is shown in Figure 12 as a function of true chlorophyll concentrations. The Case 1 water reflectance model was used. Pixel aggregation reducing the radiometric noise effects in all bands was made to the cell size of 2.6 km. The chlorophyll precision threshold and objective are also shown in the figure along with system specification. It is seen from Figure 12 that sensor predicted performance is substantially better than the sensor specification performance for high chlorophyll concentrations.
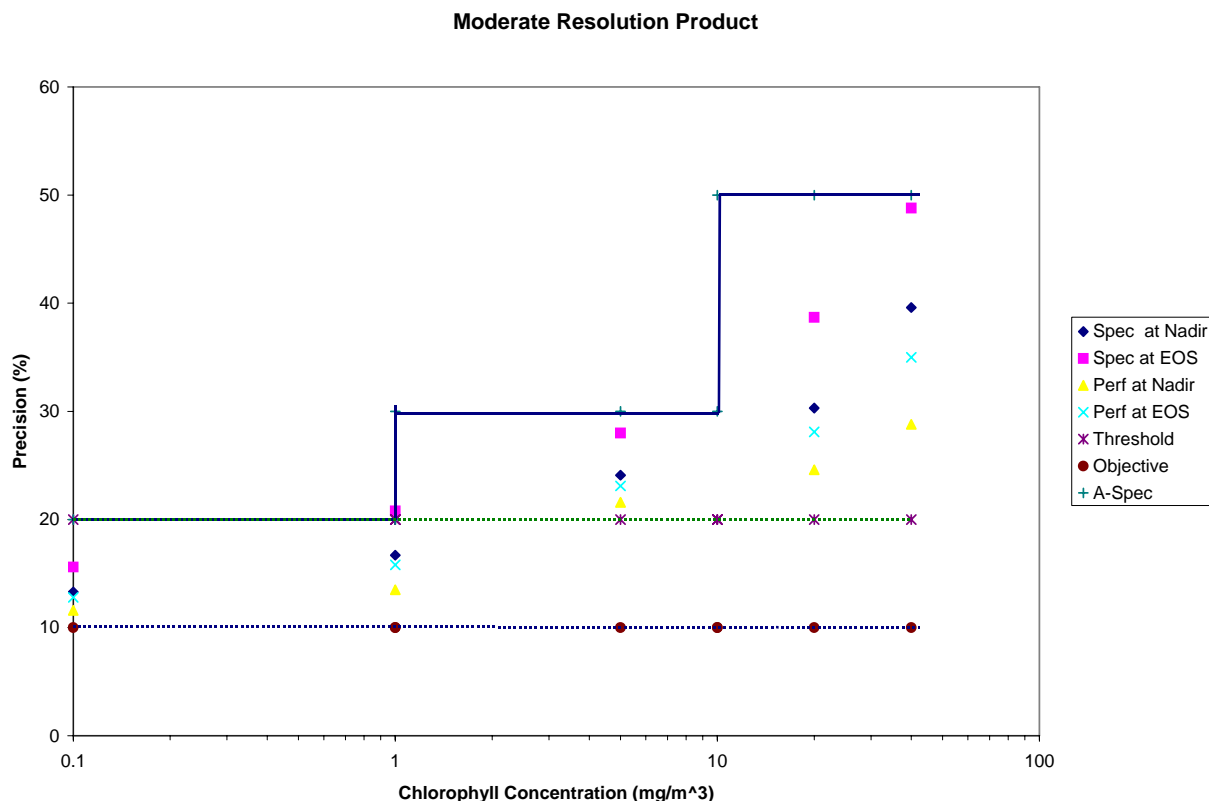
Moderate Resolution Product

Figure 12. Shows chlorophyll precision as a function of chlorophyll concentration for radiometric noise of sensor specification and predicted performance. The chlorophyll precision is shown at nadir and edge of swath (EOS). System specification is shown in a solid line.

The chlorophyll accuracy for the EDR is shown in Figure 13 as a function of true chlorophyll concentrations. The chlorophyll accuracy threshold and objective are also shown in the figure along with system specification. It is seen from Figure 13 that the sensor predicted performance is slightly better than the sensor specification performance only for high chlorophyll concentrations.
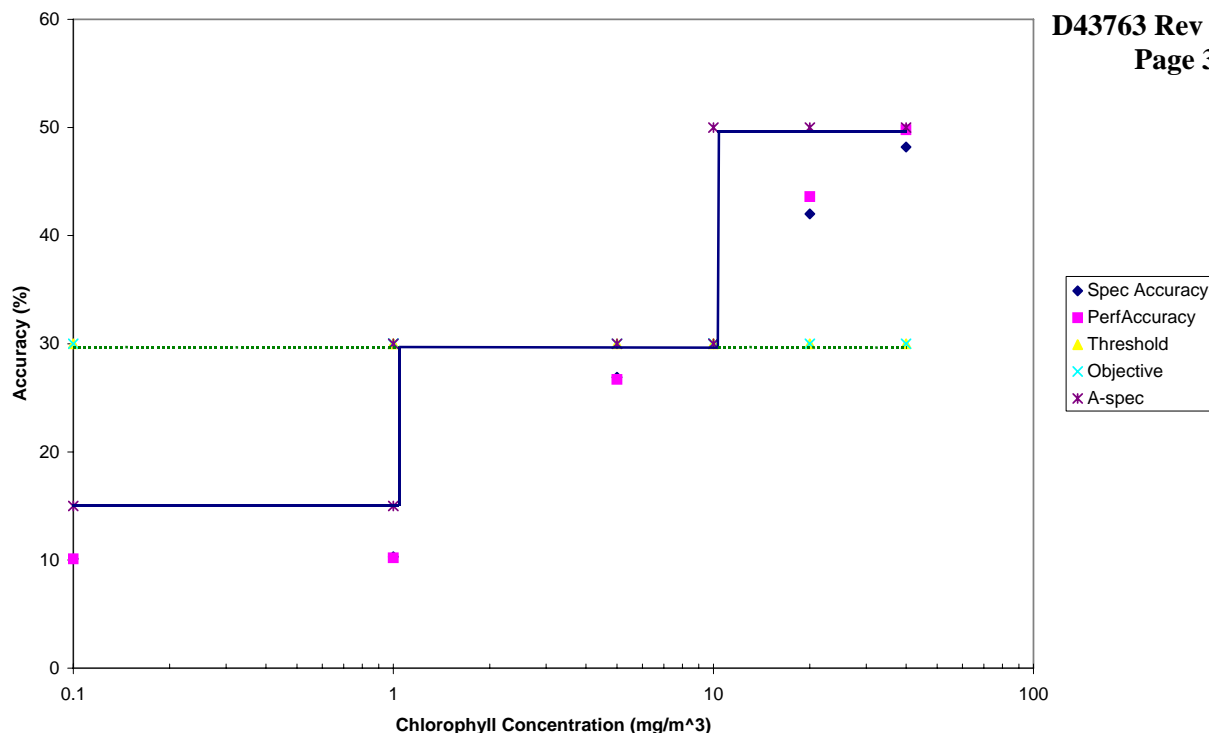
Figure 13. Shows chlorophyll accuracy as a function of chlorophyll concentration for the moderate resolution product. A-Spec is shown in a solid line.

The sediment-rich reflectance model was used for regions within 370 km of a coastline. This reflectance model has larger values of remote sensing reflectance for a given chlorophyll concentration than the reflectance model for open ocean waters. Therefore, the effects of sensor radiometric noise are smaller. Pixel aggregation of 3 by 3 at nadir was made only for the NIR bands supporting the atmospheric correction algorithm. No pixel aggregation was made for the visible bands. This approach is based on a reasonable assumption that horizontal gradients of the atmosphere are smoother than horizontal gradients of the ocean. The approach allows significant reduction of the effects of sensor radiometric noise on atmospheric correction. The chlorophyll uncertainty for the fine resolution product is shown in Figure 14 as a function of true chlorophyll concentrations. The chlorophyll uncertainty threshold is also shown in the figure along with system specification. It is seen from Figure 14 that the sensor predicted performance is quite close to the sensor specification performance for all chlorophyll concentrations.
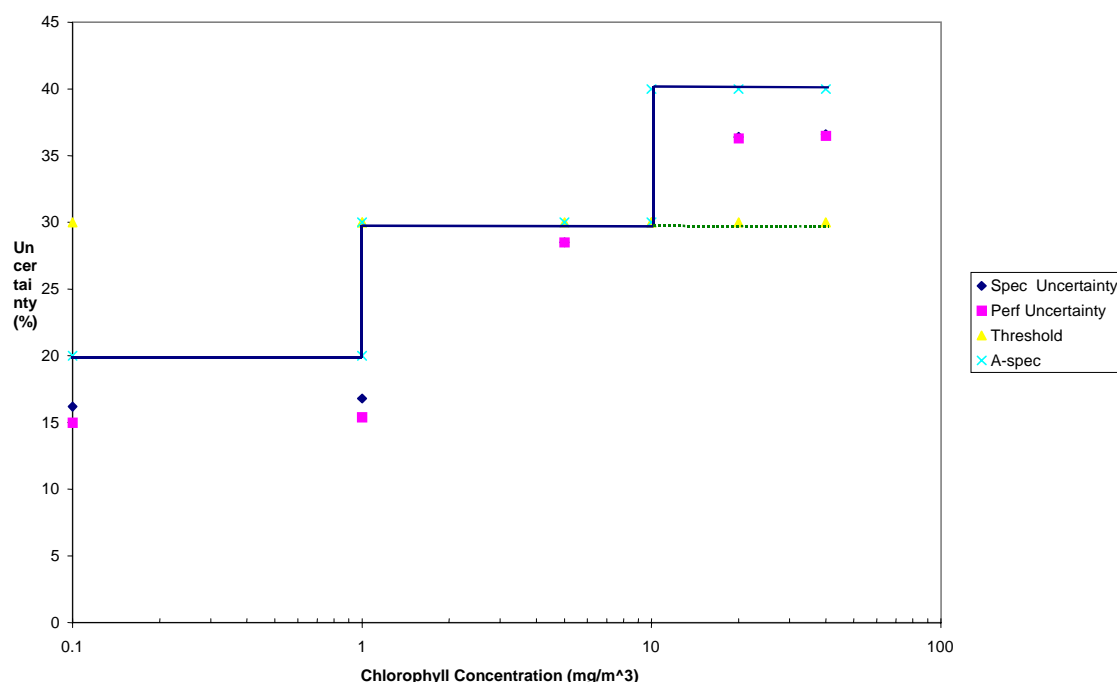
Figure 14. Shows chlorophyll uncertainty as a function of chlorophyll concentration.

3.4.5   VIIRS Specification versus SeaWiFS Performance and MODIS Specification

It is of interest to compare VIIRS system specification with specification and performance of current ocean color sensors: SeaWiFS and MODIS. Such a comparison is made in Table 11 for the similar resolutions. MODIS specification numbers were obtained from EOS Science Plan (1999). SeaWiFS performance was evaluated in Aiken et al. (1998) by a comparison of the *in situ* measured and satellite-derived chlorophyll concentrations.

Table 11 Comparison of VIIRS system specification for the moderate resolution product with MODIS specification and SeaWiFS performance

Chlorophyll (mg m⁻³)	VIIRS System Spec Accuracy, %	VIIRS System Spec Precision, %	VIIRS Uncertainty, %	MODIS Uncertainty, %	SeaWiFS Uncertainty, %
0.1≤Chl≤1.0	15	20	25	30	35
1.0<Chl≤10	30	30	42	60	worse than 35% beyond 0.05<Chl<1
10.0<Chl	50	50	70	(TBD)	

The VIIRS chlorophyll uncertainty may be improved further for high chlorophyll concentrations as part of the potential pre-planned product improvements to the algorithm performance on the basis of MODIS experience, for example, by regional adjustment of the pigment packaging parameters.

3.5   PRACTICAL CONSIDERATIONS

3.5.1   Numerical Computation Considerations

The algorithm is computationally fast and suitable for operational use.

3.5.2   Programming and Procedural Considerations

The algorithm makes use of a numerical solution of two algebraic equations. A computer code is written in ANSI C. All algorithm parameters are read in from a file.

3.5.3   Configuration of Retrievals

A configuration file is used to establish the numerical values of adjustable parameters used within the retrieval, e.g., a parameter defining whether the "packaged," "unpackaged," or "global" version of the algorithm should be used, parameters describing the normalized pigment absorption coefficient, and empirically derived constants in the empirical band-ratio algorithm used by default. This avoids specific values in the software and allows adjustment of the algorithm to specific ocean areas, such as coastal waters.

3.5.4   Quality Assessment and Diagnostics

A number of parameters and indicators will be reported in the Chlorophyll Product as retrieval diagnostics. Included among these are parameters of the configuration file and statistical information regarding the processing.

3.5.5   Exception Handling

Chlorophyll retrievals are performed only if the atmospheric correction algorithm provides positive values of water-leaving radiances in the VIIRS visible bands at 412, 445, 488, and 555 nm. If the algorithm results in chlorophyll concentrations above a predetermined maximum value, algorithm outputs will be set to –1.

3.6   ALGORITHM VALIDATION

Validation of the algorithm will rely on *in situ* measurements of spectral water-leaving reflectance and the chlorophyll *a* concentration. Please see the algorithm validation recommendation for Atmospheric Correction Over the Ocean, Y2389.

4.0 ASSUMPTIONS AND LIMITATIONS

4.1 ASSUMPTIONS

The following assumptions have been made with respect to the chlorophyll retrievals described in this document.

- Remote sensing reflectance at the VIIRS visible band wavelengths are available from the VIIRS atmospheric correction over ocean algorithm.

- Water-leaving reflectance is described as a function of the ratio of the total backscattering coefficient to the total absorption coefficient.

- The spectral slope of the DOM absorption coefficient is empirically determined.

- Parameters of the SPM backscattering coefficient are empirically correlated to the remote-sensing reflectance.

4.2 LIMITATIONS

The following limitations apply to the chlorophyll retrieval described in this document.

- Retrievals will not be performed over a pixel for which atmospheric correction fails, resulting in zero or negative water-leaving radiance in VIIRS visible bands 412, 445, 488, and 555 nm.

- This EDR will be retrieved in sun glint and shallow water regions with a poor quality label.

5.0 REFERENCES

Aas, E. (1987). Two-stream irradiance model for deep waters. *Applied Optics*, Vol. 26, 2095-2101.

Aiken J., D.G Cummings, S.W. Gibb, N.W. Rees, and et al. (1998). AMT-5 cruise report. *SeaWiFS Postlaunch Technical Report Series*, Ed. S.B. Hooker, Vol. 2, 113 p.

Antoine D., J.-M. Andre, and A. Morel (1996). Oceanic primary production. 2. Estimation at global scale from satellite (CZCS) chlorophyll. *Glob. Biochem. Cycles*, Vol. 10, pp. 57-69.

Bricaud A., A. Morel, and L. Prieur (1981). Absorption by dissolved organic matter of the sea (yellow substance) in the UV and visible domains. *Limnol. Oceanogr.*, Vol. 26, No. 1, pp. 43-53,.

Bricaud, A.M. Babin, A. Morel, and H. Claustre (1995). Variability in the chlorophyll-specific absorption coefficients of natural phytoplankton: analysis and parameterization. *J. Geophys. Res.*, Vol. 100, No. C7, 13,321-13,332.

Burenkov, V.I., A.P. Vasilkov, and L.A. Stephantsev (1985). Retrieval of spectral inherent optical properties of seawater from the spectral reflectance. *Oceanology*, Vol. 25, No. 1, 49-54.

Carder, K.L. (2004). High spectral resolution MODIS algorithms for ocean chlorophyll in case II waters. *NAS5-31716*.

Carder, K.L., F.R. Chen, J.P. Cannizzaro, J.W. Campell, B.G. Mitchell (2004). Performance of the MODIS semi-analytical ocean color slgorithm for chlorophyll-*a. Advances in Space Research,* Vol. 33, 1152-1159.

Carder, K.L., F.R. Chen, Z. Lee, S.K. Hawes, and J.P. Cannizzaro (2003). MODIS: Case 2 chlorophyll *a* algorithm. MODIS ATBD-19, URL http://modis.gsfc.nasa.gov/data/atbd/atbd_mod19.pdf.

Carder, K.L., F.R. Chen, Z.P. Lee, S.K. Hawes, and D. Kamykowski (1999). Semi-analytical MODIS algorithm for chlorophyll a and CDOM absorption with bio-optical domains based on nitrate-depletion temperatures. *J. Geophys. Res.*, Vol. 104, No. C3, 5,403-5,421.

Carder, K.L., S.K. Hawes, K.A. Baker, R.C. Smith, R.G. Steward, and B.G. Mitchell (1991). Reflectance model for quantifying chlorophyll *a* in the presence of productivity degradation products. *J. Geophys. Res.*, Vol. 96, 20, 559-20, 611.

Doerffer, R., and J. Fisher (1994). Concentrations of chlorophyll, suspended matter, and gelbstoff in case II waters derived from satellite coastal zone color scanner data with inverse modelling methods. *J. Geophys. Res.*, Vol. 99, No. C4, 7,457-7,4660.

EOS Science Plan (1999). Ed. M.D. King. Raytheon ITSS Publication, 397 p.

Garver, S.A. and D.A. Siegel (1997). Inherent optical property inversion of ocean color spectra and its biogeochemical interpretation: 1. Time series from the Sargasso Sea. *J. Geophys. Res.*, Vol. 102, 18,607-18,625.

Golubitskiy, B.M. and I.M. Levin (1980). Transmittance and reflectance of layer of highly anisotropic scattering medium. Izvestiya USSR Academy of Sciences, *Atmospheric and Oceanic Physics*, Vol. 16, 926-931.

Gordon H.R., and A. Morel (1983*). Remote assessment of ocean color for interpretation of satellite visible imagery. A review.* New York: Springer.

Gordon, H.R. (1973). Simple calculation of the diffuse reflectance of the ocean. *Applied Optics,* 12, 2803-2804.

Gordon, H.R. (1989). Dependence of the diffuse reflectance of natural waters on the sun angle. *Limnology and Oceanography*, Vol. 34, 1484-1489.

Gordon, H.R., D.K. Clark, J.W. Brown, O.B. Brown, R.H. Evans, and W.W. Broenkow (1983). Phytoplakton pigment concentrations in the Middle Atlantic Bight: Comparison of ship determinations and CZCS estimates. *Applied. Optics*, Vol. 22, No. 1, 20-36.

Gordon, H.R., and M. Wang (1994). Retrieval of water-leaving radiance and aerosol optical thickness over the oceans with SeaWiFS: a preliminary algorithm. *Applied Optics*, 33, 445-450.

Gordon, H.R. (1997). In-orbit calibration strategy for ocean color sensors. *Remote Sens. Environ.*, Vol. 63, 265-278.

Haltrin V.I., and G.W. Kattawar (1993). Self-consistent solutions to the equation of transfer with elastic and inelastic scattering in oceanic optics: I. Model. *Applied Optics*, Vol. 32, 5,356-5,367.

Hoge, F.E., and P.E. Lyon (1996). Satellite retrieval of inherent optical properties by linear matrix inversion of oceanic radiance models: an analysis of model and radiance measurement errors. *J. Geophys. Res.*, Vol. 101, No. C7, 16,631-16,648.

Hucks, J. (1998). RSTX Internal Memorandum Y1629.

Kamykowski, D. (1987). A preliminary biophysical model of the relationship between temperature and plant nutrients in the upper ocean. Deep-Sea Research, Vol. 34, No. 7, 1067-1079.

Kirk, J.T.O. (1984). Dependence of relationship between inherent and apparent optical properties of water on solar altitude. *Limnol. Oceanogr.*, Vol. 29, 350-356.

Lee, Z., K.L. Carder, S.K. Hawes, R.G. Steward, T.G. Peacock, and C.O. Davis (1994). Model for the interpretation of hyperspectral remote-sensing reflectance. *Appl. Opt.*, Vol. 33, No. 24, 5,721-5,732.

Lee, Z., K.L. Carder, T.G. Peacock, C.O. Davis, and J.L. Mueller (1996). Method to derive ocean absorption coefficients from remote-sensing reflectance. *Appl. Opt.*, Vol. 35, No. 3, 453-462.

Liu, Q. and E. Rupert (1996). A radiative transfer model: matrix operator method. *Applied Optics*, Vol. 35, 4229-4237.

McClain C.R., M.L. Cleave, G.C. Feldman, W.W. Gregg, and S.B. Hooker (1998). Science quality SeaWiFS data for global biosphere research. Sea Technology, Vol. 39, No. 9, 10-16.

Maritorena, S. (1998). Personal communication.

Miller S. (1998) Raytheon Internal Memorandum 98VIIRSL00026.

Morel, A. (1988). Optical Modelling of the Upper Ocean in Relation to Its Biogenous Matter Content (Case 1 Waters). *J. Geophys. Res.*, Vol. 93, 10,749-10,768.

Morel, A. (1996). Optical properties of oceanic Case 1 waters, revisited. *Ocean Optics* XIII, Proceedings SPIE, Vol. 1963, 108-113.

Morel, A., and B. Gentili (1993). Diffuse reflectance of oceanic waters. II. Bidirectional Aspects. *Applied Optics*, 32, 6864.

Morel, A., and L. Prieur (1977). Analysis of variations in ocean color. *Limnology and Oceanography*, Vol. 22, 709-722.

O'Reilly, J.E., S. Maritorena, B.G. Michell, D.A. Siegel, K.L. Carder, S.A. Garver, M. Kahru, and C.McClain (1998). Ocean color chlorophyll algorithms for SeaWiFS. *Journal of Geophysical Research*, Vol. 103, 24,937-24,953.

O'Reilly, J.E. (2000).

Pope, R.M., and E.S. Fry (1997). Absorption spectrum (380-700 nm) of pure water. II. Integrating cavity measurements. *Applied Optics*, Vol. 36, 8,710-8,723.

Roesler, C.S., and M.J. Perry (1995). In situ phytoplankton absorption, fluorescence emission, and particulate backscattering spectra determined from reflectance. *Journal of Geophysical Research*, Vol. 102, 13,279-13,294.

Smith, R.C., and K.S. Baker (1981). Optical properties of the clearest natural waters (200-800 nm). *Appl. Opt.*, Vol. 20, No. 2, 177-183.

Sogandares, F.M., and E.S. Fry (1997). Absorption spectrum (340-700 nm) of pure water. I. Photothermal measurements. *Applied Optics*, Vol. 36, 8,710-8,723.

Sugihara, S., M. Kishino, and N. Okami (1985). Estimation of water quality parameters from irradiance reflectance using optical models. *J. Oceanog. Soc. Japan*, Vol. 41, 399-406.

Tassan, S. (1994). Local algorithms using SeaWiFS data for the retrieval of phytoplankton pigments, suspended sediment, and yellow substance in coastal waters. *Applied Optics,* Vol. 33, 2369-2378.

Vasilkov, A.P. (1997). A retrieval of coastal water constituent concentrations by least-square inversion of a radiance model. *Proceedings of the 4th International Conference on Remote Sensing for Marine and Coastal Environments*, Orlando, Florida, 17-19 March 1997, Vol. II, 107-116.

Vasilkov, A.P., and L.A. Stephantsev (1987). Effect of solar elevation in remote measurements on the spectral composition of radiation exiting from the ocean. *Oceanology*, Vol. 27, No. 2, 163.

Vermote, E.F., D. Tanré, J.L. Deuzé, M. Herman, and J.J. Morcrette (1997). Second simulation of the satellite signal in the solar spectrum, 6S: An overview. *IEEE Trans. Geosci. Remote Sensing*, Vol. 35, 672.

Zaneveld, J.R.V. (1982). Remotely sensed reflectance and its dependence on vertical structure: a theoretical derivation. *Applied Optics*, Vol. 21, 4,146-4,150.